Universidade de Aveiro
2014

Departamento de Electrónica, Telecomunicações e
Informática

Clara Maria
Apolinário
Lucas da Silva

Desenho de amplificadores de baixo ruído para Radioastronomia

Low Noise Amplifiers' Design for Radioastronomy

"..but of course I ask for the impossible, if I have asked for the possible I would be empty-handed..."

— anonymous

Universidade de Aveiro
2014

Departamento de Electrónica, Telecomunicações e Informática

Clara Maria Apolinário Lucas da Silva

Desenho de amplificadores de baixo ruído para Radioastronomia

Low Noise Amplifiers' Design for Radioastronomy

Universidade de Aveiro Departamento de Electrónica, Telecomunicações e Informática
2014

Clara Maria Apolinário Lucas da Silva

Desenho de amplificadores de baixo ruído para Radioastronomia

Low Noise Amplifiers' Design for Radioastronomy

Dissertação apresentada à Universidade de Aveiro para cumprimento dos requesitos necessários à obtenção do grau de Mestre em Engenharia Electrónica e Telecomunicações , realizada sob a orientação científica do Professor Doutor Luís Filipe Mesquita Nero Moreira Alves , Professor Auxiliar do Departamento Electrónica, Telecomunicações e Informática da Universidade de Aveiro

Dedico este trabalho aos meus pais
I dedicate this work to my parents

o júri / the jury

presidente / president

Professor Doutor João Nuno Pimentel da Silva Matos
Professor Associado do Departamento de Electrónica, Telecomunicações e Informática da Universidade de Aveiro

vogais / examiners committee

Doutor Luis Manuel Santos Rocha Cupido
Diretor Executivo, Lc Technologies

Professor Doutor Luis Filipe Mesquita Nero Moreira Alves
Professor Auxiliar do Departamento de Electrónica, Telecomunicações e Informática da Universidade (Orientador)

agradecimentos / acknowledgements

Bem, por onde começar... Sem sombra de dúvida pelos meus pais. Foram eles o meu maior apoio, foram eles que não permitiram que eu desistisse do meu sonho e tudo fizeram para que eu o concretizasse, foram eles o melhor exemplo que eu podia seguir.
Não podia deixar de referir também os meus orientadores neste projecto, Professor Luis Nero e em especial o Miguel Bergano que acabou por se tornar um amigo. Sem a ajuda, a paciência, o esforço e o empenho dele, este projecto teria sido muito mais difícil para mim. Obrigada Miguel pelo tempo que perdeste comigo e pelas palavras de encorajamento que me fizeram acreditar nas minhas capacidades. Professor Nero a si agradeço-lhe a sua boa disposição e acima de tudo a sua exigência e insistência no rigor e qualidade do meu trabalho. E claro a sua calma e serenidade que constrasta em tudo com a minha personalidade irrequieta e nervosa.
Ao longo deste trajecto houve várias pessoas que me acompanharam uma delas foi sem dúvida o Joel Dinis. Obrigada pelas tuas palavras de melhor amigo e que mesmo quando tinha vontade de mandar tudo pelos ares soubeste me acalmar e dar um novo ânimo.
Não podia também deixar de agradecer ao pessoal do meu laboratório de CSI. André, Gonçalo, Mónica e Frederico obrigada por terem tornado tudo mais leve e divertido.
Claro que tenho de agradecer também ao meu amor, Sporting ensinaste-me a ter sempre esperança. E por fim gostaria de agradecer a todas as bandas que me fizeram companhia nesta longa caminhada.

Palavras-chave Radioastronomia, radiofrequência, radiometria, amplificador de baixo ruído

Resumo A exploração do espaço sempre foi uma ambição do ser humano. Hoje em dia as novas tecnologias aplicadas na área de radioastronomia tornaram possível que esta última meta ficasse cada vez mais atingível.
O reforço fornecido pelas grandes empresas que produzem o equipamento e os componentes necessários, impulsionou o avanço de novos projectos grandiosos tais como o SKA. No âmbito deste projecto arrojado apresenta-se esta dissertação com o intuito de estabelecer uma nova aproximação à implementação de recentes tecnologias no desenho de amplificadores de baixo ruído.
O enquadramento deste trabalho bem colmatar a necessidade de diminuir o custo dos vários componentes que integram os sistemas de recepção. O amplificador de baixo ruído está inserido no radiómetro, que, após a antena, é o primeiro dispositivo a ser alcançado pela radiação electromagnética proveniente do espaço. A importância da construção de um amplificador que introduza um nível de ruído baixo com um custo reduzido deve-se principalmente à quantidade massiva destes elementos num projecto desta envergadura e à necessidade da sua qualidade ter de ser elevada para garantir a consequente descodificação do sinal recebido.

Keywords Radioastronomy, radio frequency, radiometer, low noise amplifier

Abstract Space exploration has always been an ambition to human kind. Nowadays the new technologies that could be used in radioastronomy field have made this goal even more attainable.
The big manufacturers that produce the equipment and the necessary components have made a big reinforcement that boosted the creation of new colossal projects, such as the SKA. Within this bold project stands this thesis with the intention of establishing a new approach to the implementation of the recent technologies on the design of low noise amplifiers. This work has the objective of filling the need of decreasing the cost of the numerous components that incorporate the reception's systems. The low noise amplifier is inserted on the radiometer which follows the antenna and is the first electronic device reached by the electromagnetic radiation coming from space. The construction's importance of an amplifier that introduces a low level of noise at reduced cost is due to the massive amount of this type of elements that exists on a project of this magnitude. It is also due to the high quality that this device must have to assure the consequent decoding that follows.

Contents

List of Figures

List of Tables

Constant Designation	**Symbol**	**Constant Value**	**Units**
Boltzmann	k_B *or* k	1.381×10^{-23}	JK^{-1}
		8.617×10^{-5}	eVK^{-1}
Planck	h	6.626×10^{-34}	Js
		4.136×10^{-15}	eVs
Speed of light	c	2.998×10^{8}	ms^{-1}
		1.079×10^{9}	kmh^{-1}
Jansky	Jy	1×10^{-26}	$Wm^{-2}Hz^{-1}$
		1×10^{-23}	$ergHz^{-1}s^{-1}cm^{-2}$
Vacuum permeability	μ_0	$4\pi \times 10^{-7}$	NA^{-2}
Vacuum permittivity	ε_0	8.854×10^{-12}	Fm^{-1}

Table 1: Table of constants

Acronyms

ADS Advanced Design System. 2, 31, 32, 44, 46, 49, 51–53, 55, 62, 65, 67, 68

ASKAP Australian Square Kilometer Array Pathfinder. v, 6

BJT Bipolar Junction Transistor. 14

DC Direct Current. 48, 49, 57, 58, 62

DUT Device Under Test. 61, 62

EM Electromagnetic. 5, 8

ENR Excess Noise Ratio. 59

FET Field Effect Transistor. 14, 15, 18, 29

HEMT High Electron Mobility Transistor. 1, 14, 30, 67

HF High Frequency. 6

HJ-FET Hetero Junction Field Effect Transistor. 31, 44

IC Integrated Circuit. 14

LNA Low Noise Amplifier. 1, 2, 10, 13, 25–30, 32, 42, 44, 46, 49, 51–53, 57, 58, 62, 65, 67, 68

MLIN microstrip Line. 47, 49, 53

MLOC Microstrip Line Open Circuit stub. 49, 53

MMIC Monolithic Microwave Integrated Circuit. 46, 47

MN Matching Network. 20, 21, 24, 25, 31, 32, 34, 36, 37, 39, 40, 42, 44, 46, 47, 55

MOSFET Metal Oxide Semiconductor Effect Transistor. 14, 15

MTEE Microstrip T-junction. 49

NF Noise Figure. 25, 26, 28–31, 36, 37, 39, 42, 44, 46–49, 51–53, 57–59, 61, 62, 64, 65

PCB Printed Circuit Board. 22, 57

pHEMT pseudomorphic High Electron Mobility Transistor. 14

RF Radio Frequency. 1, 2, 10, 13, 18, 20, 28–31, 44, 46, 48, 49, 52, 55, 58, 62, 64, 67

SETI Search for Extraterrestrial Intelligence. 4

SKA Square Kilometre Array. 1, 4

SMA SubMiniature version A. 48, 62

TEM Transverse Electromagnetic. 22

UHF Ultra High Frequency. 6

VHF Very High Frequency. 6

Chapter 1

Introduction

1.1 Motivation

The advanced technologies that have recently appeared in the market, have rose the question: is it possible to build a reliable Low Noise Amplifier (LNA) at a cheaper price? Providing an answer to this question has become the main motivation for this dissertation. The major companies and manufacturers of Radio Frequency (RF) technology have contributed with transistors and other components capable of operating at high frequencies with low noise introduction to the overall system.

The case of study for this work is the High Electron Mobility Transistor (HEMT) and their variants (pseudomorphic and metamorphic). Their characteristics and advantages (concerning the noise) when compared to other types of transistors, made them a preferred choice for this assignment.

An inherent subject to the objective of this work is the Square Kilometre Array (SKA) project. The development of new scientific knowledge, the search for outer space activity and the need of satisfying millennial unanswered questions, made this ambitious project to involve millions of euros. The detection of faint signals, demands an unpaired quality when compared to other existing systems. Thus LNA can be priced on thousands of euros. The price also rises due to the cryogenic temperatures that are in the surrounding system to prevent noise increase.

This academic work is an effort to explain the reader of the difficulties and the elements that must be taken into consideration when designing a LNA for radioastronomy receivers.

1.2 Main goals

The main goals that are intended to be achieved are the following:

- Research of recent technologies that are capable of being used at RF, and contemporary technology that is being used.

- Study and investigation of the HEMT transistors that can be used on the construction of a LNA.

- Simulation of different aspects that are crucial to the implementation of any microwave amplifier.
- Design of a LNA capable of operating at RF with low noise introduction and competitive enough to be considered on the current market.
- Analysis and interpretation of the results that were obtained.
- Pertinent conclusions to the overall project.

1.3 Dissertation structure

Throughout this document there will be a description of most of the theoretical concepts that are used to obtain the objectives that are proposed. This allows any reader to fully understand the work that was taken.

The second chapter is a thorough explanation of all the theoretical background that is needed to fully understand what is behind the construction of a LNA. It has also an approach to the state of the art, and where the LNA technology stands at this point in time.

In chapter three there is an introduction and presentation of the simulations developed that contributed to the design and implementation of the LNA. The software used was MATLAB (version R2013a) of Mathworks company and Advanced Design System (ADS) (version 2012.08) of Agilent company.

The forth chapter presents the results obtained after the construction of the LNA. With the help of tables and figures it is possible for the reader to understand the accomplishments that were made.

The fifth chapter is a reproduction of the conclusions of the global work and proposal of a future work that can be taken by others that follow. An overview of the improvements that can be made is also present at this chapter.

Chapter 2

Theoretical background

2.1 Summary

In this chapter there is a presentation of all the theoretical concepts that act as supporting material for the practical part of this work. There is also an overview of the current technology that exists at the market.

2.2 Radio Astronomy

Astronomy is probably the most ancient of sciences. Since the early years of humankind, the universe was always considered to be filled with mysteries and a source of legends and superstitions. The hunger for new knowledge and the pursuit of revealing some of the universe's secrets, drove people throughout centuries of history, to research and develop solutions that could provide the tools and the means to obtain these goals. On the timeline of astronomy's history there are scientists like Galileo Galilei, Isaac Newton, Albert Einstein, Carl Sagan, Stephen Hawking...among others, for whom we should all be grateful for their breakthrough discoveries that made modern astronomy possible.

2.2.1 Brief history

Radio astronomy is a branch of astronomy that studies radio emissions from celestial bodies. One of its pioneers was radio engineer Karl Guthe Jansky. While he was making a study research for the Bell Telephone Laboratories, he stumbled upon a signal unknown to the date. He later realize that this statical signal came from the Milky Way Galaxy. Cosmic radio waves were discovered and a new era rose for other researchers to continue Karl Jansky's work [10]. After reading the discoveries of Karl Jansky, electronics engineer Grote Reber, constructed the first parabolic reflector radio telescope (Figure 2.1). He was able to make the first sweep of radio waves of the sky [11].

During the second world war there was a big investment in the development of radar systems which helped support the evolution of radio astronomy. Another scientist that gave a big contribution to radio astronomy was John Kraus. Not only he is the author of some renowned publications, as he is also the founder and designer of the Ohio

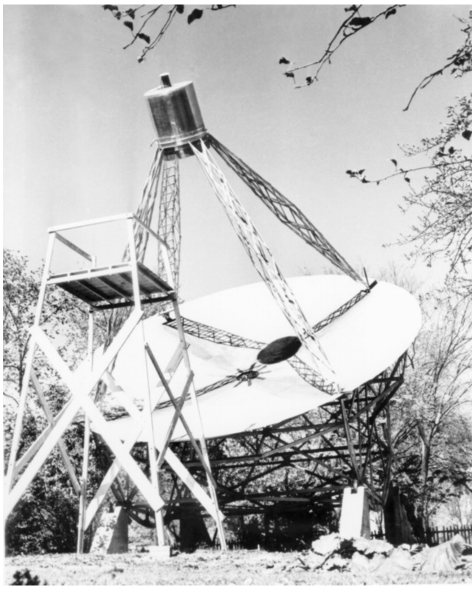

Figure 2.1: First radio telescope [1].

State University Radio Observatory, home of the Big Ear. This facility made part of the Search for Extraterrestrial Intelligence (SETI) project, and is best known for the detection of the WOW! signal. It was destroyed in the late 90's, but its existence had a huge influence on the future of radio astronomy [12] [13].

The SKA is one of the most ambitious and challenging projects that involves scientists and researchers from all around the world. The main goal is to obtain the biggest and most sensitive radio telescope ever built that will have the power and ability to explore all of the electromagnetic spectrum and even beyond it. To conquer this goal that massive project will be an array of coherently connected antennas spread over an area about 300 km in extent with an aggregate antenna collecting area of up to 106 m^2 at centimeter and meter wavelengths[14], holding three types of receivers: dishes, low frequency telescopes and mid frequency telescopes. The project is being developed in phases and it is located in South Africa and Australia [15].

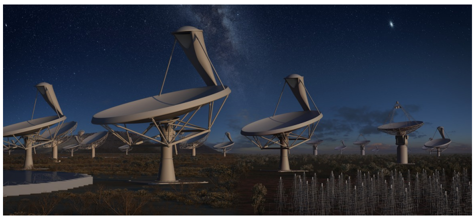

Figure 2.2: Artists rendition of the SKA Dish arrays in operation at night time [2].

2.2.2 Theoretical concepts

For a better understanding of the science and methods behind the collection of data from space, one must first comprehend some concepts of interest.

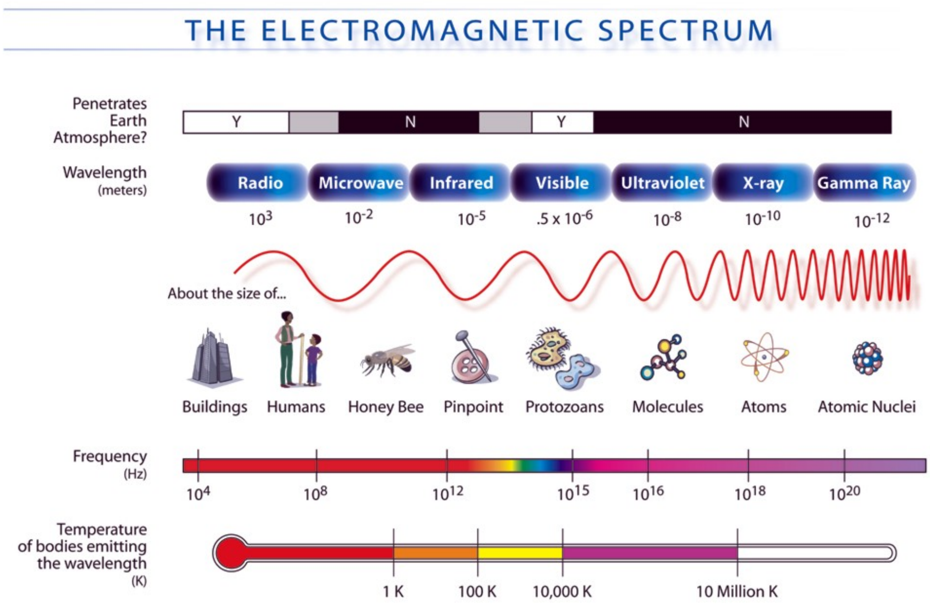

Figure 2.3: Electromagnetic spectrum [3].

Electromagnetic spectrum

The electromagnetic waves travel at the speed of light and their frequency (ν) and wavelength(λ) are characterized by the following expression:

$$c = \lambda\nu \qquad (ms^{-1}) \tag{2.1}$$

As it is possible to see from the previous equation the wavelength is inversely proportional to the frequency. So if a wave has a high frequency its wavelength will be low and vice-versa. The energy can be obtained with the aid of the Planck's constant, and with the use of the following expression [16]:

$$E = h\nu \qquad (J) \tag{2.2}$$

The previous expression proves that the energy is directly proportional to the frequency. The higher the frequency, the higher the energy associated to that specific wave.

Figure 2.3 displays the EM spectrum and some of its characteristics. The diagram shows that there is a relation between the temperature and the frequency (or energy) of a wave, more about this subject will be explained on a forward subsection.

The designations given by the IEEE for the radar frequencies' bands are displayed on Table 2.1.

Antennas

Antennas are used for both emission and reception of Electromagnetic (EM) waves. Some of the parameters that best describes their performance are: the radiation pat-

Designation	Frequency	Wavelength
High Frequency (HF)	3 to 30 MHz	100 to 10 m
Very High Frequency (VHF)	30 to 300 MHz	10 to 1 m
Ultra High Frequency (UHF)	300 to 1000 MHz	100 to 30 cm
L Band	1 to 2 GHz	30 to 15 cm
S Band	2 to 4 GHz	15 to 7.5 cm
C Band	4 to 8 GHz	7.5 to 3.75 cm
X Band	8 to 12 GHz	3.75 to 2.5 cm
Ku Band	12 to 18 GHz	2.5 to 1.67 cm
K Band	18 to 27 GHz	1.67 to 1.11 cm
Ka Band	27 to 40 GHz	1.11 to 0.75 cm
V Band	40 to 75 GHz	7.5 to 4.0 mm
W Band	75 to 110 GHz	4 to 2.7 mm
mm Band[1]	110 to 330 GHz	2.7 to 1.0 mm

Table 2.1: IEEE Standard Letter Designations for Radar-Frequency Bands [9].

tern, the beam width, the radiation power density, the radiation intensity, the directivity, the efficiency, the gain and the polarization [17] [18] [19].

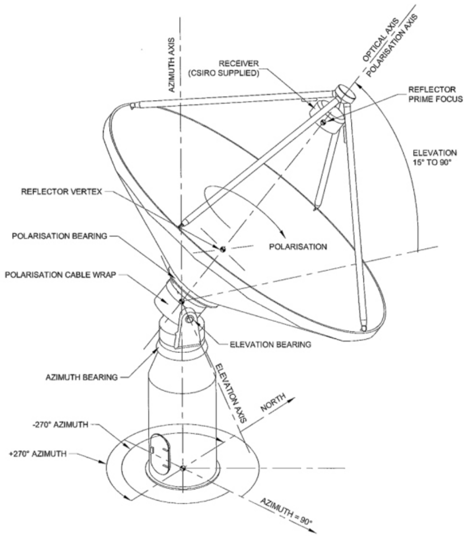

Figure 2.4: ASKAP's antenna diagram [4].

When dealing with a receiving antenna, the measure that needs to be taken is the flux density of a radio emission's source. This relates the power received (P) from a specific area of collection (A) with the bandwidth (B) and the efficiency of the antenna (η) (Equation 2.3)

$$S = 2\frac{P}{\eta AB} \quad (Wm^{-2}Hz^{-1}) \tag{2.3}$$

The units for the flux density are the ones showed on Equation 2.3, but in radio astronomy it is common to use the Jansky (Jy) also as a tribute to Karl Jansky.

[1] millimeter wave

Another useful concept is the surface brightness (or intensity) of the source, that can be described by the following equation [20]:

$$B_\nu(T) = \frac{2h\nu^3/c^2}{e^{h\nu/kT} - 1} \quad (WHz^{-1}m^{-2}Sr^{-1}) \tag{2.4}$$

h is the Planck's constant
ν is the frequency
c is the velocity of light in vacuum
k is the Boltzmann's constant
T is the temperature in Kelvins

The previous equation is also called the Planck's function. The flux density can also be described by the integration of the Planck's function over a solid angle [20]

$$S = \int B(\nu)d\Omega \quad (Wm^{-2}Hz^{-1}) \tag{2.5}$$

The power received by the antenna can be characterized by the following equation:

$$P = kT_AB \quad (W) \tag{2.6}$$

T_A is the antenna's temperature (not physically) that aggregates all the temperatures from the surroundings (sky, atmosphere, humans, amongst others). The relation between temperature and noise and its importance is a well known fact among astronomers, and for a better understanding of this subject an extended explanation will be given at subsection 2.2.3.

Black body radiation

The black body is an important concept used on the analysis of the transfer of electromagnetic waves and thermal radiation. It is used as a standard of comparison with the object of study. The black body, ideally, absorbs all types of radiation that focus over it and consequently reflects no energy. The black body radiation is the result of it being in thermal equilibrium (at a constant temperature). Some of its properties are quite helpful, it is isotropic and homogeneous, it only depends of the temperature (at a given wavelength) and it is the strongest when compared with others at the same temperature. The brightness temperature given by equation 2.7 is a way to express the temperature of a blackbody in thermal equilibrium that is equivalent to the temperature of the object of study in the same equilibrium [20] [21].

$$T_b = \frac{B_\nu(T)C^2}{2k\nu^2} \quad (K) \tag{2.7}$$

Remote sensing

Even though an object could be light-years way, its electromagnetic radiation can still wander throughout space and reach the antenna's range of a radio telescope on earth. Remote sensing is the collection of that radiation and with so the extraction of all the information regarding the object of study without physical approach. The process of remote sensing involves various features that must be considered and some are going to be expose here [21]:

- The object of study must provide EM energy.
- When the EM radiation reaches Earth the passage through different mediums weakens the signal and may cause its distortion.
- The interaction with the source provides an analysis of its geometrical characteristics that is encrypted in the EM radiation.
- The process that involves the reception is carried out by sensors on satellites that orbit Earth or on terrestrial radio telescopes.
- Those sensors are attached to electronic devices that convert the EM radiation into an electronic signal that can then be processed.
- The receiving stations carries out the processing and stacking of the signal that will be later handled by experts.

Radiometry

All matter can be modeled as energy composed by charged particles. When some sort of external excitement (temperature modifications) occurs there is a variation in the motion of the particles which provides an alteration to the energy perceptible by the electromagnetic waves radiated. This radiation is mainly composed by a considerable number of independent waves at distinct frequencies that are most commonly known as noise. Radiometry is the process that involves the measurement of that radiation. Some notions, that sometimes cause confusion, are useful to understand and are exposed in the diagram of figure 2.5.

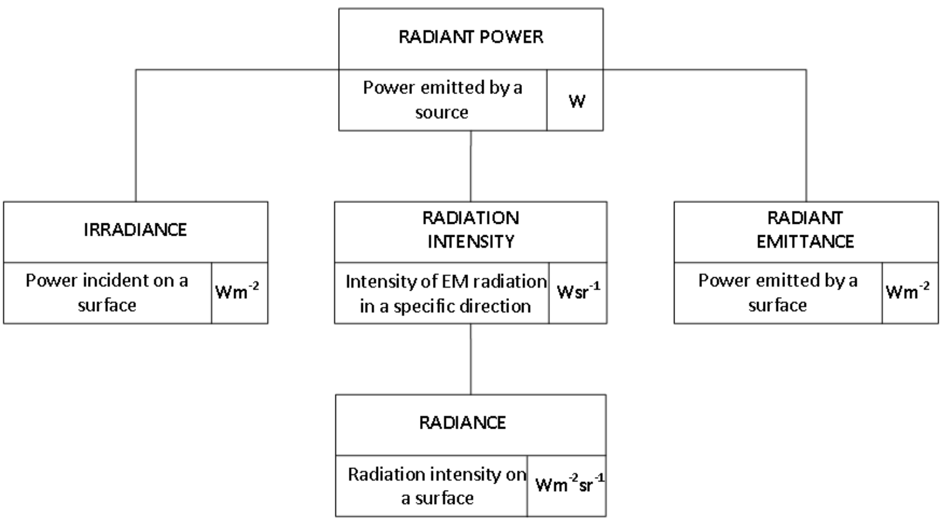

Figure 2.5: Radiometry concepts.

2.2.3 Noise

Noise is an inherent characteristic to all electrical devices, it can be defined as disturbances that interferes in the reception of a real and desired signal that is being transmitted. Any body that is at a temperature above 0 K emanates noise energy due to the random motion of the electrons that constitute their material. In all signals that are transmitted and received, noise is present and makes its contribution. There are many types of noise, but for this case of study they are not as important or relevant as the ones that are going to be mentioned [22] [23].

Categories of noise:

- Thermal noise also known as Johnson-Nyquist noise is the most elemental form of noise and is associated to the irregular agitation of the charged particles of the electrical material caused by thermal variations, hence its name.
- Shot noise is associated to the charge carriers of components with semiconductor's junctions like diodes and transistors.
- Flicker noise or pink power density spectrum is mostly perceived at lower frequencies and is the main source of noise on DC amplifiers at higher frequencies it is camouflaged by other types of noise.

A method that is used to calculate the noise is the one which makes the assumption that a system's noise can be equivalent to a resistor that would present equal characteristics. Having that in mind, the following expression determines the noise voltage (V_N) caused by a noisy resistor (R_N) [24]:

$$V_N = \sqrt{4kTBR_N} \tag{2.8}$$

R_N is the noisy resistor in Ohms (Ω)
k is the Boltzmann's constant
T is the temperature in degrees Kelvin of the noisy resistor (K)
B is the bandwidth of the system in Hertz (Hz)

The maximum power available from this noisy resistor can be calculated by the following expression:

$$P_N = \frac{V_N^2}{4R_N} = kTB \tag{2.9}$$

There are three common ways to describe quantitatively the noise of a system:

Designation	**Symbol**	**Units**
Noise Factor	F	Dimensionless
Noise Figure	NF	dB
System Noise Temperature	T_{sys}	K

Table 2.2: Quantitatively representation of the noise.

The subsequent expressions supply the mathematical description of the above items:

$$SNR = \frac{Power\ of\ the\ signal}{Power\ of\ the\ noise} \tag{2.10}$$

$$F = \frac{input\ SNR}{output\ SNR} = \frac{P_{si}/P_{ni}}{P_{so}/P_{no}} = \frac{P_{no}}{G_A P_{ni}} \tag{2.11}$$

$$F = \frac{kBT_{out}}{kBT_{in}G_A} = \frac{T_{out}}{T_{in}G_A} \tag{2.12}$$

$$NF = 10\log_{10} F \tag{2.13}$$

$$T_{sys} = (F-1)T_0 \tag{2.14}$$

T_0 is the standard room temperature (290 K)

2.2.4 Radio-telescope

Figure 2.6: Radio-telescope [5].

The radio-telescope (Fig. 2.6) has a main role on the study of space. It is a powerful device capable of receiving radio wave emissions from outer space. Its operation range can be from 30 MHz to 300 GHz. It is composed mainly by two parts: a large radio antenna and a sensitive radio (or radio receiver). In Fig. 2.7 there is a conceptual description of the signal's path since it reaches the antenna till it is analyzed on a computer. The first electronic device to be reached by the radio emissions is a RF amplifier, the LNA. This device should be as close as possible to the antenna so that there is a minimization of the losses produced by the feed line. Another reason for the LNA to be that near of the antenna is since the received signal has traveled such a long distance and has passed through different mediums it becomes too weak and some how degraded and there is a demand for amplifying it first.

2.2.5 Radiometer receiver

The radiometer receiver is a device whose main purpose is to measure the radiated power of a source. When dealing with some specific microwave applications it is more advantageous and efficient to express this power in terms of an equivalent temperature.

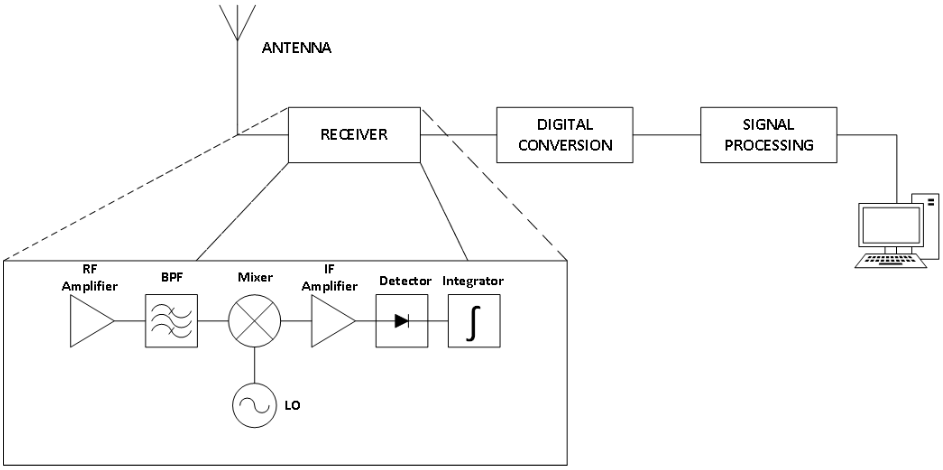

Figure 2.7: Radio-telescope : conceptual block diagram.

The concept behind this instrument is the following: an antenna is pointing to an radiating object, the signal is captured and the task now is to find a relation between both of them (Fig.2.8). The antenna's temperature (T_A) is the sum of all the temperatures

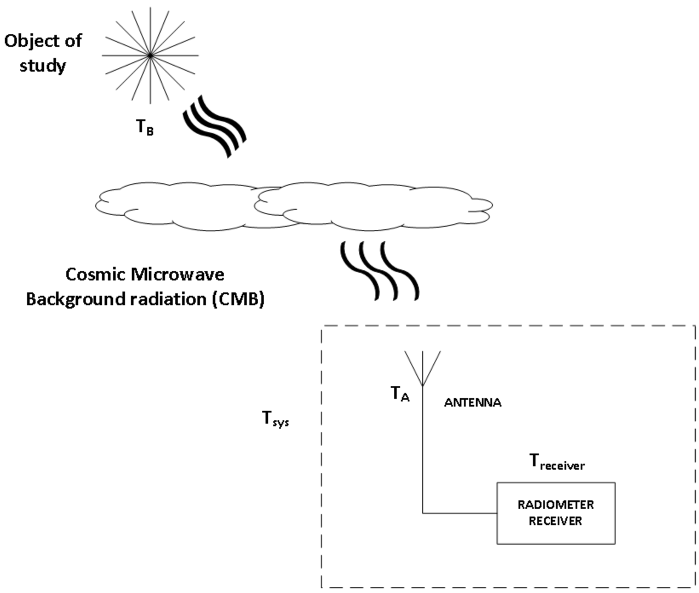

Figure 2.8: Drawing of the procedure for measuring the brightness temperature.

of the elements that reaches the antenna. This means that it is a collection of all the noise temperatures associated with Earth and its surroundings added to the one that is being studied (T_B). After being received by the antenna, the next device to be reached by the signal is the radiometer receiver. This device will also add a noise temperature ($T_{receiver}$) to the overall value, and unfortunately it will be much higher when compared to T_A. Therefor

$$\begin{aligned} T_A &= T_B + T_{others} \\ T_{sys} &= T_A + T_{receiver} = T_B + T_{others} + T_{receiver} \end{aligned} \tag{2.15}$$

Having in consideration that studies have already been conducted that calculates the temperatures of most of the elements that are constant (T_{others}) [25], and that the $T_{receiver}$ is also possible to be calculated, the remain temperature will be the object's (T_B). The values of T_B are relatively small when compared to T_A so the challenge on the design of the radiometer receiver is to make sure it has a good sensitivity to make it possible to distinguish both in order to obtain the correct value of T_B [26] [27].

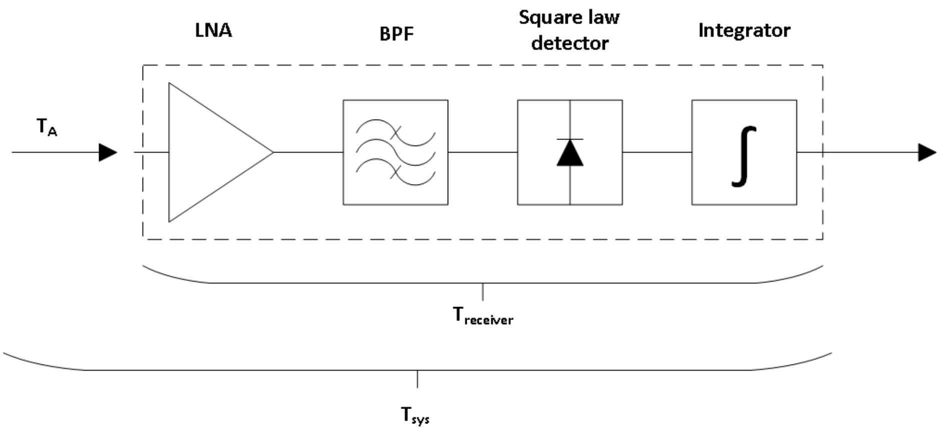

Figure 2.9: Total power radiometer - block diagram.

The radiometer is nevertheless a measurement instrument with certain specifications that must be mentioned for a better understanding:

- Accuracy is the capability of the instrument to provide a measure as close as possible to the real value.
- Precision provides a notion of the instrument's stability by evaluating the deviation of different measures of the same input value.
- Resolution is the minimum value of change in the input that the instrument can detect at the output.
- Sensitivity is the smallest amount of signal that the instrument can measure.

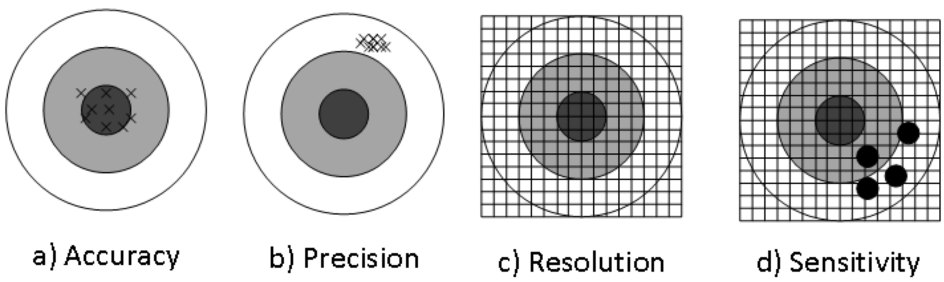

Figure 2.10: Accuracy, precision, resolution and sensitivity.

For a better understanding of these concepts that sometimes causes confusion, figure 2.10 depicts a similar situation with a target. The analogy is simple: accuracy is making measures as close as possible to the real value, precision is making measures that are always consistent and similar (even though not being close to the real value). The biggest confusion is between resolution and sensitivity. As it is possible to see the difference is that even though the resolution provides a small value for the distinct measures, the sensitivity locks that value to a minimum that may not match the resolution's value. This way sensitivity is one of the most important characteristic of the radiometer.

So in short, at the input of the radiometer receiver there is T_{sys}. To know what the output of the radiometer will be, one most first understand the processing of the input signal through all its components. Taking a look at Fig. 2.9, the first block that appears is an amplifier (LNA). This component provides the gain to the radiometer by amplifying the signal. To prevent the excessive addition of noise to the system the LNA is usually cryogenically cooled (reducing its temperature the noise produced by it is also reduced). The following block is a band pass filter centered at a determined frequency with a specific bandwidth. Its function is to eliminate all the information that falls out of the desired band. The next block is a square law detector. Its function is to rectify the incident signal providing only the envelope wave that surrounds the signal. This way only the intensity of the input radio wave will be processed in the following stages. The last step of the radiometer receiver will be an integrator, its function is to smooth the variations of the signal. The longer the integration time, the smoother the signal gets [26] [27].

As it has been mentioned before, the sensitivity of the radiometer receiver is one of its most important characteristics. The quality of this attribute makes it possible to distinguish the small value of the T_B that is included in the T_A, which are all included in the total value of the T_{sys}. For the radiometer depicted on figure2.9 the formula that provides the result of the output is the following one [26]:

$$V_{OUT} = kBG(T_{sys}) \tag{2.16}$$

For the sensitivity of this type of radiometer the formula that provides a result is the one that follows [26]:

$$\Delta T = \frac{T_{sys}}{\sqrt{B\tau}} \tag{2.17}$$

This formula is a result of mathematical calculations that will not be exposed in this document. τ is the time of integration as for B stands for the bandwidth used. The sensitivity of the radiometer depends on T_{sys}, B and τ. The integration time is the only element of this equation which is possible to be changed, although with some limitations. A high value of τ corresponds to a decrease of the value of the sensitivity, which provides the quality necessary to measure the value of T_B.

2.3 Amplifier

The first stage of the radio receiver, as it has been mentioned, is a RF amplifier. There are many types of amplifiers and circuits to obtain them, mostly by using transistors. The most common transistors are the three-terminal semiconductor devices:

Bipolar Junction Transistor (BJT) and Field Effect Transistor (FET) with their variants. Within the FETs the most commonly used is the Metal Oxide Semiconductor Effect Transistor (MOSFET) and for this case of study the focus will be on HEMT and mainly on pseudomorphic High Electron Mobility Transistor (pHEMT).

2.3.1 Transistors

BJTs were widely used for decades in all sorts of electronic devices. The characteristics of a MOSFET turned it gradually smaller when compared to a BJT. For that reason, the MOSFET is nowadays a preferred choice in the design of Integrated Circuit (IC). By having the possibility of packing a large number of MOSFETs in a single IC, the quality and the capacity of the device that is being implemented increases (it is the case of memories or processors). Some construction differences of both transistors are depict on figure 2.11 [28].

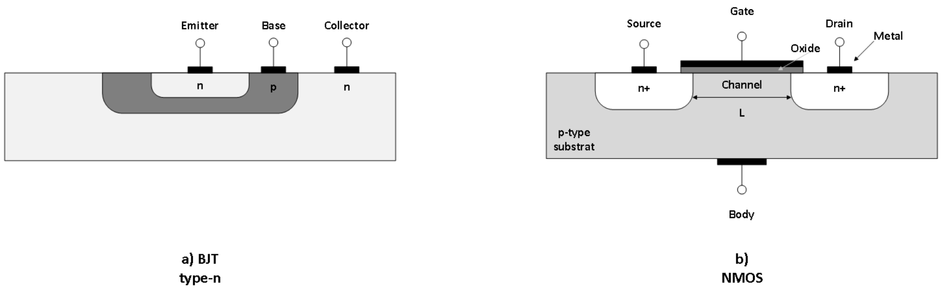

Figure 2.11: Cross-section of type-n BJT and a NMOS.

Other differences concerning the properties of both transistors: MOSFET are voltage driven devices,while BJT are current driven devices. MOSFET devices have higher input impedance and lower power dissipation and most important of all for this case of study, lower noise when compared to the BJT.

The HEMT is a variant of the FET that was implemented by Takashi Mimura [29]. Their main differences resides on the structure and the materials that are used. Their properties of low noise and high gain at radio frequencies made them the preferred transistor for low noise applications. At figures 2.12 it is possible to see both structures of the HEMT and of the pHEMT.

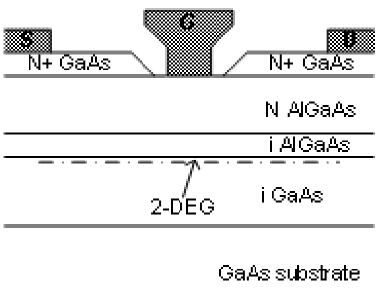

(a) Conventional HEMT.

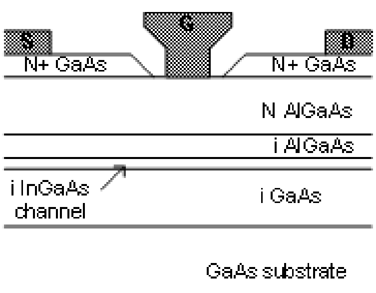

(b) pHEMT.

Figure 2.12: Structure of the HEMT and pHEMT [6].

2.3.2 Commercial transistors

Nowadays the technology of some manufacturers made it possible to have commercial transistors at a low price that can operate and have a good performance at higher frequencies. The values shown on Table 2.3 were obtained at a frequency test of 12 GHz at 298.15 K . All of the transistors displayed are best suitable for low noise applications. G_A is the available gain, more on this subject will be best analyzed on subsection 2.6.1.

Designation	Technology description	NF_{min} (dB)	G_A (dB)
VMMK-1218	GaAs pHEMT	0.84	9.95
ATF-36077	GaAs pHEMT	0.5	12
MGF4953A	GaAs HEMT	0.4	13
MGF4941AL	GaAs HEMT	0.35	13
NE3516S02	n-channel GaAs HJ-FET	0.35	14
NE3511S02	n-channel GaAs HJ-FET	0.3	13.5

Table 2.3: Low noise transistors available on the market.

2.3.3 Configurations

Making the MOSFET a general case for the FET family, it is easier to continue the study of the amplifier. There are three basic configurations for the MOSFET, each with its own utility and function. Its characteristics are shown at Table 2.4. The common-source is the most commonly used configuration and it is widely used on gain stages due to its medium voltage and current gain. The signal is introduced on the gate and exits inverted on the drain. The common-gate is not so much used as the previous configuration but it can be implemented as a current buffer or as a voltage amplifier. The power gain is the lowest when compared to the other configurations. The common-drain (also known as source follower) is commonly used for voltage buffers. Its low output impedance makes it to be a preferred choice for output stages on more complex amplifiers.

2.4 Radio Frequency analysis

When dealing with radio frequencies, there are some aspects of the components that can not be neglected like in lower frequencies. Usually the model used for these components is an ideal model and not a real one that describes every feature. The components that are used in the design of a circuit can be divided in to two major groups: the passive and the active components.

2.4.1 Passive components

The passive components are the ones that does not require an external source of energy to operate. This means that there is no special operation mode for the

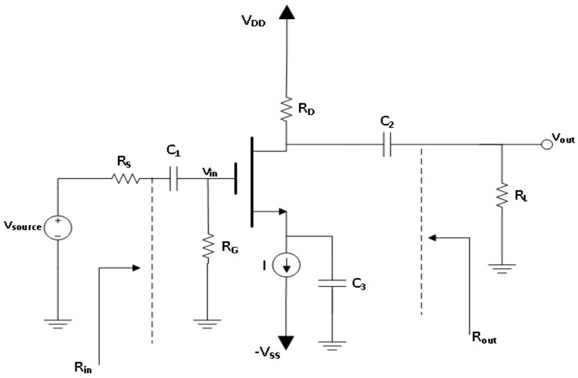 **Common-Source**	• Z_{IN} MEDIUM • Z_{OUT} MEDIUM • A_v MEDIUM • A_i MEDIUM • A_p HIGH • I/O phase=180º
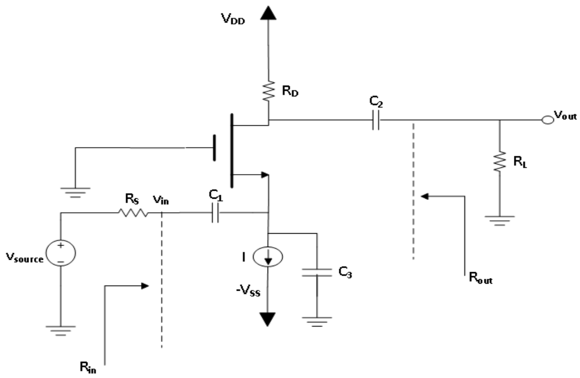 **Common-Gate**	• Z_{IN} LOW • Z_{OUT} HIGH • A_v HIGH • A_i LOW • A_p LOW • I/O phase=0º
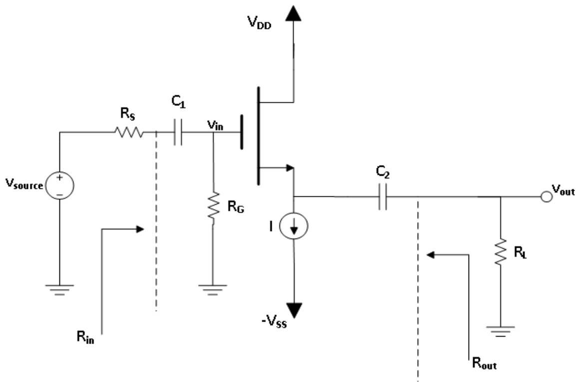 **Common-Drain**	• Z_{IN} HIGH • Z_{OUT} LOW • A_v LOW • A_i HIGH • A_p MEDIUM • I/O phase=0º

Table 2.4: Commonly used configurations.

component to work. They can either be lossy (such as resistors) or lossless (such as capacitors and inductors).

As it is possible to see at figure 2.13 there are several parasitic elements when using a simple passive component. Those elements will affect the results of the design of any device at radio frequencies. For that reason there are manufacturers that provide optimized passive components so that they do not interfere as much in the bandwidth that they are intended to be used.

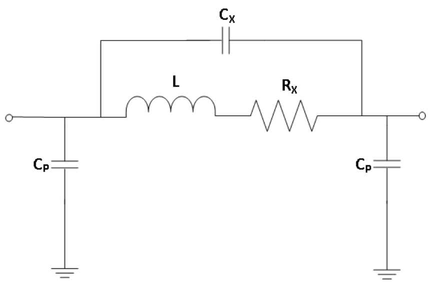

(a) Model of a real capacitor.

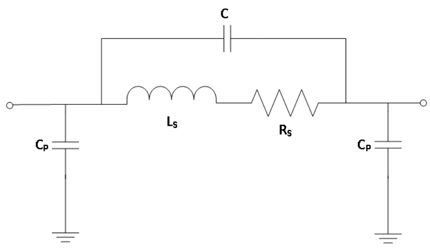

(b) Model of a real inductor.

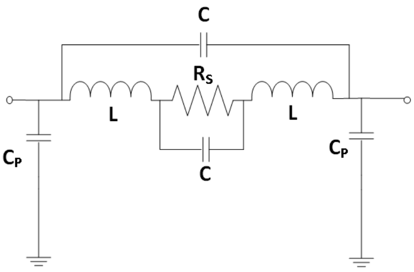

(c) Model of a real resistor.

Figure 2.13: Models at RF.

2.4.2 Active components

Active components are the ones that require an external source for their operation, in other words this means that for the component to work there must be a source that supplies the necessary energy. These components also have an important part on the circuit because they use the energy supplied on them to operate over the input signal (for example to amplify it). Components such as diodes or transistors require a determined mode of operation to work (or be active).

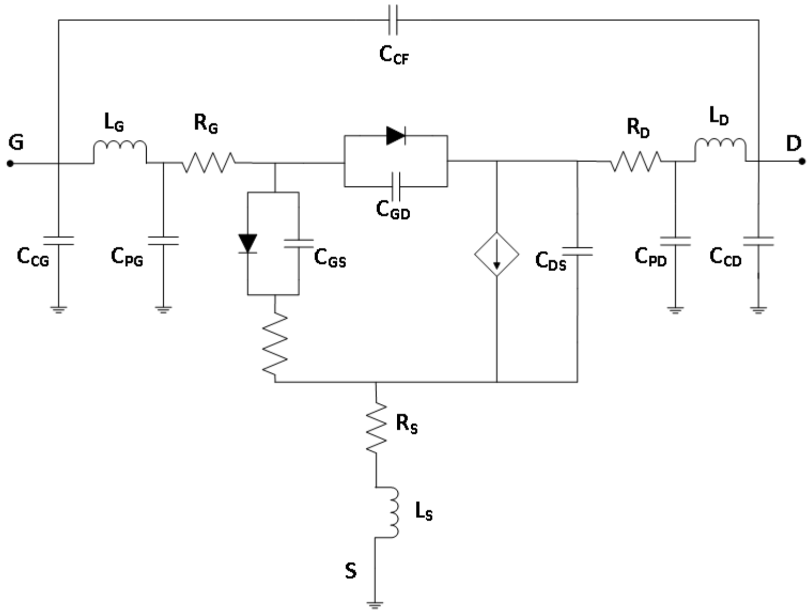

Figure 2.14: Model of a FET at RF.

In figure 2.14 it is possible to see the numerous parasitic elements associated with an active component, in this case a FET. They will have undesired effects on the outcome of the design, and they must be considered when planning any device at radio frequencies.

2.4.3 Scattering parameters

The scattering parameters are defined by a matrix that describes the properties, characteristics and behavior of a multi-port network when a radio frequency signal reaches it. The two-port network (Fig.2.15) will be the case of study throughout this document. The S-parameters are a necessary mean when dealing with RF because it is quite difficult to make tests with the transistors at this frequencies using the normal standards such as open and short circuits [24][30].

Before making the analysis of figure 2.15 one must first have in consideration the following expression:

$$\rho_x = \frac{Z_x - Z_0}{Z_x + Z_0} \tag{2.18}$$

Equation 2.18 is a simple generic representation of the reflection coefficient. The letter 'x' can be replaced by either L or S in order to obtain the load or source coefficient reflection respectively. This representation may be a very straightforward way of dealing with the reflective coefficient, but yet effective to understand what follows:

a_1 is the incident wave at the input of the two-port network generated by the source. It can also be the result of a reflection from the source. If $a_1 = 0$ then there is no reflection at the source meaning that $\rho_S = 0$ and by equation 2.18 it is possible to conclude that $Z_S = Z_0$. This has the meaning that the input is properly terminated.

b_1 is the reflected wave from the input of the two-port network. It can also be the incident wave at the source.

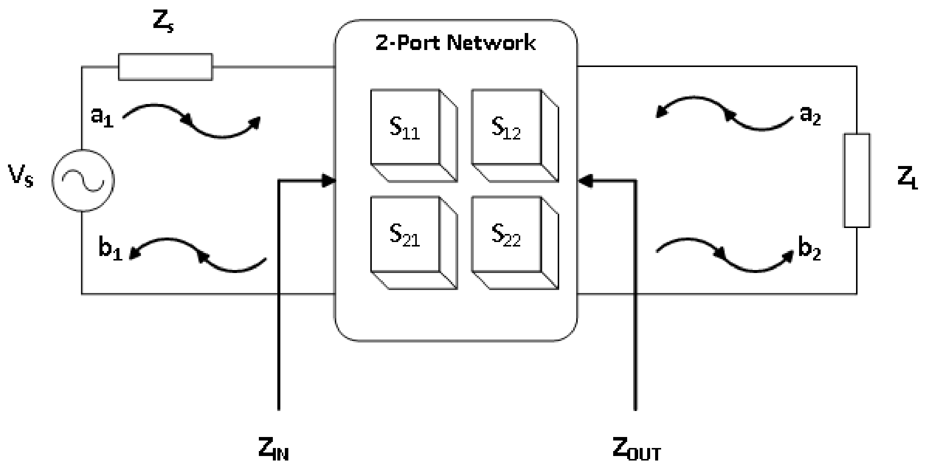

Figure 2.15: Two port network.

a_2 is the incident wave at the output of the two-port network. it can also be the wave reflected from the load. If $a_2 = 0$ then there is no reflection at the load meaning that $\rho_L = 0$ and by equation 2.18 it is possible to conclude that $Z_L = Z_0$. This has the meaning that the output is properly terminated.

b_2 is the reflected wave from the output of the two-port network. It can also be the incident wave at the load.

The following expressions concentrate the principal properties of the scattering parameters of a two port network:

$$\begin{bmatrix} b_1 \\ b_2 \end{bmatrix} = \begin{bmatrix} S_{11} & S_{12} \\ S_{21} & S_{22} \end{bmatrix} \begin{bmatrix} a_1 \\ a_2 \end{bmatrix} \tag{2.19}$$

$$\begin{aligned} b_1 &= a_1 S_{11} + a_2 S_{12} \\ b_2 &= a_1 S_{21} + a_2 S_{22} \end{aligned} \tag{2.20}$$

$$S_{11} = \frac{b_1 - a_2 S_{12}}{a_1} \quad \text{if } a_2 = 0 \quad S_{11} = \frac{b_1}{a_1} \tag{2.21a}$$

$$S_{12} = \frac{b_1 - a_1 S_{11}}{a_1} \quad \text{if } a_1 = 0 \quad S_{12} = \frac{b_1}{a_2} \tag{2.21b}$$

$$S_{21} = \frac{b_2 - a_2 S_{22}}{a_1} \quad \text{if } a_2 = 0 \quad S_{21} = \frac{b_2}{a_1} \tag{2.21c}$$

$$S_{22} = \frac{b_2 - a_1 S_{21}}{a_2} \quad \text{if } a_1 = 0 \quad S_{22} = \frac{b_2}{a_2} \tag{2.21d}$$

Taking into count the result of equation 2.21a it is possible to conclude that when the output is properly terminated, S_{11} becomes the ratio between the reflected wave and the incident wave at the input and it is designated as the input reflection. It is also a parameter that can represent the accuracy of the input matching.

With the result of equation 2.21b it is possible to conclude that with the input properly terminated S_{12} is the ratio between the reflected wave at the input with the incident wave at the output. This is the transmission that occurs from the output to the input and hence is designated by reverse transmission.

The result of equation 2.21c is similar to the previous one in this case is the ratio between the reflected wave at the output with the incident wave at the input, S_{21} becomes a representation of the transmission from the input to the output (also called forward transmission) when the output is properly terminated.

Finally it is possible to observe from the result of equation 2.21d that S_{22} is the ratio between the reflected and the incident wave at the output. This parameter represents the output reflection and can also express the accuracy of the output matching.

2.4.4 Maximum Power Transfer

The ideal transmission of a signal between a generator (source) and a load suffers no reflections in the intermediate stages, however most of the times that is quite difficult to take place due to the impedance mismatches that occurs on the transmission lines and on the components inserted on the circuit. Those discrepancies evolve into a loss on the power gain and an increase of the noise figure. Also the reflections that occur on the circuit may damage the components or even the generator. Considering all of this, obtaining a maximum power transfer becomes an important goal on the design of any microwave device and that is possible with the help of matching networks on the input and on the output (more on this subject will be presented on section 2.5).

Taking into count figure 2.15, the condition to obtain an impedance matching is that the real part (resistance) should be equal to the real part of the termination that is being treated (source or load) and its complex part (reactance) should be equal on magnitude but with opposite sign. This is called the complex conjugate matching. Expressions 2.23 and 2.22 shows the basic principle of this subject [24].

$$Z_{in} = Z_S^* \tag{2.22}$$

$$Z_{out} = Z_L^* \tag{2.23}$$

To prevent reflections caused by mediums with different impedance levels which causes losses on the transmission of RF signals, the conditions that must be taking into consideration are related with the reflection coefficients.

$$\Gamma_{in} = \Gamma_S^* \tag{2.24}$$

$$\Gamma_{out} = \Gamma_L^* \tag{2.25}$$

Γ_{in} is the reflection coefficient at the input of the two port network.
Γ_{out} is the reflection coefficient at the output of the two port network.
Γ_L is the reflection coefficient at the load.
Γ_S is the reflection coefficient at the source.

2.5 Matching Networks

The Matching Network (MN) are a solution to the mismatches mentioned on subsection 2.4.4. Figure 2.16 is a representation of the set of matching networks that

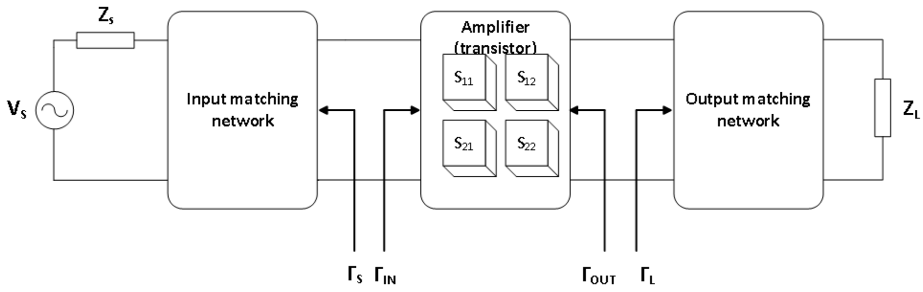

Figure 2.16: Matching networks of an amplifier.

are required to guarantee the conditions of expressions 2.24 and 2.25 that provides a maximum power transfer between a source and a load.

At figure 2.16 it is possible to observe that the amplifier's information is given by the s-parameter matrix. It is with that information that both input and output MN are configured. The matching networks can either be designed with lumped elements or transmission lines. One of the methods to obtain the values for each component of the MN is with the aid of a Smith Chart.

2.5.1 Lumped elements

There are many forms to perform a matching network with lumped elements. Figure 2.17 shows some of the viable variants.

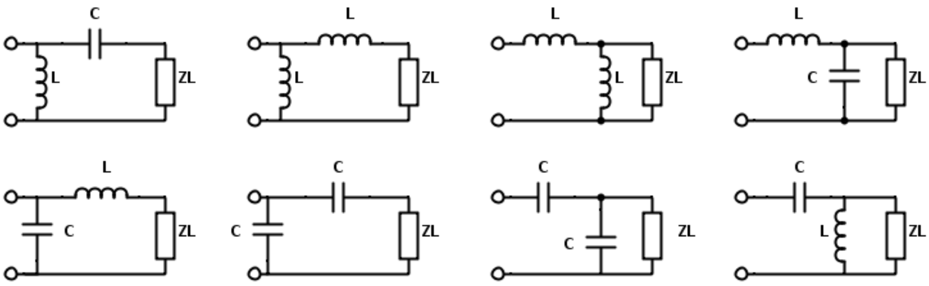

Figure 2.17: Matching networks with lumped elements.

Although quite simple and effective at low frequencies, these type of matching networks fail to succeed at higher frequencies. This is due to the fact that each lumped component (as is has been mentioned previously at subsection 2.4.1) is affected with other parasitic elements. Their overall effect traduces into problems with the noise and the gain performance of the amplifier. An alternative for their use are transmission lines.

2.5.2 Microstrip lines

The manufacturing of circuits have come a long way since the first printed circuit board (PCB) was made by Paul Eisler [31]. The advantages that it brought for the designs and implementations of electronic circuits made it crucial for the innovations that followed. Nowadays it is possible to implement any type of circuit for any type of signal, in a cheaper and easy way. There are many types of transmission lines that can be used on Printed Circuit Board (PCB). Unfortunately they are also a cause of losses and noise interference to the signal. Microstrip lines due to their top notch performance are preferred for microwave applications. Microstrip lines consists of a conductor strip that lays on a dielectric substrate that separates it from the ground plane [32]. Figure 2.18 depicts a simple representation of the microstrip and its features.

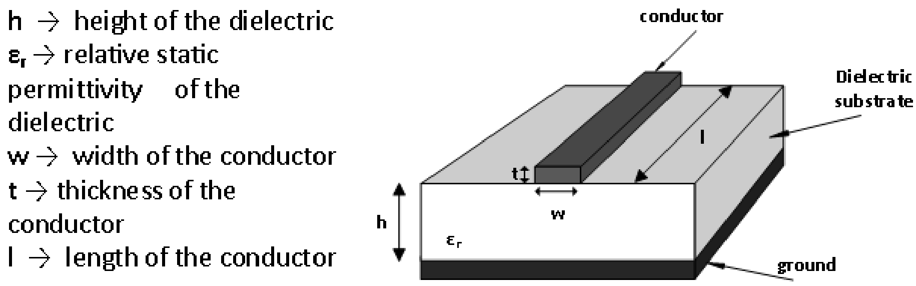

Figure 2.18: Microstrip cross-section.

The dielectric constant makes the propagation waves to go slower because of their quasi-Transverse Electromagnetic (TEM) characteristic. TEM occurs when the medium of propagation is the air but since in microstrip lines the dielectric is not the air but a material with different ε_r the electric and the magnetic waves are not orthogonal to each other as it is suppose to be. This is referred to as quasi-TEM. However at very high frequencies the non orthogonality of the waves becomes worst and the reference of quasi-TEM is no longer valid.

The parameters that best describes the behavior associated to the microstrip are the following:

$$\Lambda = \frac{\lambda_0}{\sqrt{\varepsilon_{eff}}} \tag{2.26}$$

The expression 2.26 is the representation of the wavelength in the microstrip line. ε_{ff} is the effective dielectric constant which depends of the physical dimensions of the microstrip line and of the ε_r of the dielectric used.[32][18]

For the calculation of ε_{eff} the most accurate formula was developed by Hammerstad and Jensen [33] (Equation 2.28).

$$u = \frac{W}{h} \tag{2.27}$$

Where W stands for the width of the conductor and h for the height of the dielectric.

$$\varepsilon_{eff} = \frac{\varepsilon_r + 1}{2} + \frac{\varepsilon_r - 1}{2}\left(1 + \frac{10}{u}\right)^{-ab} \tag{2.28}$$

The values of a and b are obtained by the following expressions:

$$a = 1 + \frac{1}{49}\ln\left(\frac{u^4 + \left(\frac{u}{52}\right)^2}{u^4 + 0.432}\right) + \frac{1}{18.7}\ln\left(1 + \left(\frac{u}{18.1}\right)^3\right) \tag{2.29}$$

$$b = 0.564\left(\frac{\varepsilon_r - 0.9}{\varepsilon_r + 3}\right)^{0.053} \tag{2.30}$$

The characteristic impedance of the line is determined by the following expressions:[33]

$$f(u) = 6 + (2\pi - 6)\mathrm{e}^{\left(-\left(\frac{30.666}{u}\right)^{0.7528}\right)} \tag{2.31}$$

$$\eta_0 = \sqrt{\frac{\mu_0}{\varepsilon_0}} \tag{2.32}$$

$$Z_0 = \frac{\eta_0}{2\pi\sqrt{\varepsilon_{eff}}}\ln\left(\frac{f(u)}{u} + \sqrt{1 + \frac{4}{u^2}}\right) \tag{2.33}$$

Another parameter associated with a microstrip line is the width of the conductor. This value is calculated in function of the ratio of expression 2.27 [24][18][34]. If the value of $u \leq 2$ then one must first calculate the value of A on equation 2.34 and then substitute this value on equation 2.35.

$$A = \frac{Z_0}{\eta_0}\pi\sqrt{2(\varepsilon_r - 1)} + \frac{\varepsilon_r - 1}{\varepsilon_r + 1}\left(0.23 + \frac{0.11}{\varepsilon_r}\right) \tag{2.34}$$

$$u = \frac{8}{\mathrm{e}^{A} - 2\mathrm{e}^{-A}} \tag{2.35}$$

If the value of $u > 2$ then one must first calculate the value of B at equation 2.36 and substitute this value on expression 2.37

$$B = \frac{\eta_0\pi}{2Z_0\sqrt{\varepsilon_r}} \tag{2.36}$$

$$u = \frac{2}{\pi}\Big(B - 1 - \ln(2B - 1)\Big) + \frac{\varepsilon_r - 1}{\pi\varepsilon_r}\left(\ln(B - 1) + 0.39 - \frac{0.61}{\varepsilon_r}\right) \tag{2.37}$$

The value of h is provided by the manufacturers and the value of W is finally obtained by expression 2.27. The process that involves the calculation of ε_{eff} and Z_0 is called analysis and the one that involves the calculation of W is called synthesis.

Figure 2.19 shows some of the possibilities with the use of elements of microstrip lines.

2.5.3 Smith chart

Smith chart is a method developed by Phillip H. Smith. This graphical aid makes it possible to visualize the impedance of an element at different frequencies [35]. The Smith chart is a transformation between an impedance and the reflection coefficient

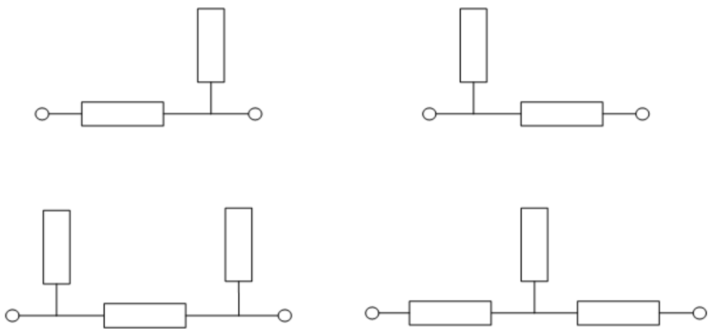

Figure 2.19: Matching networks with microstrip elements.

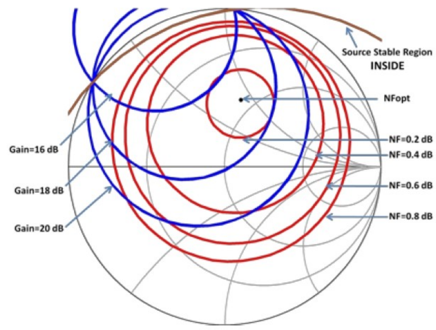

Figure 2.20: Constant circles drawn on the Smith Chart [7].

of a transmission line [30]. With this tool it is possible to calculate the elements of the MN. If they are composed with lumped elements it can be used to calculate the values of the capacitors and of the inductors. If in other hand they are constructed with microstrip lines, it is possible to calculate the values of the dimensions of the lines and of the stubs that are used.

Another help that this tool provides is the compromise that one must take between the gain and the noise figure. For that there is the constant gain and noise figure circles drawn on the Smith chart. Those circles identify the areas where the gain and the noise figure are constant and with so one can make a choice of what values to use on the elements that compose the MN.

2.5.4 Input matching network

When performing the configuration of an input matching network one must take into count the main goal of it. The following formula is the one that best describes the considerations that must the be taken when configuring the input matching network [24] :

$$\Gamma_{IN} = S_{11} + \frac{S_{12} S_{21} \Gamma_L}{1 - S_{22} \Gamma_L} \tag{2.38}$$

It is possible to see that Γ_{IN} is influenced by Γ_L. If either that value or S_{12} are equal to zero then the previous expression takes the form that follows:

$$\Gamma_{IN} = S_{11} \tag{2.39}$$

This expression is related to an unilateral amplifier. This concept stands for the situation where the amplifier only has the capacity to transmit through one way (forward transmission) and with so only has forward power gain. Using the mathematical approach, this means that the S_{12} (expression 2.21b) (reverse transmission coefficient) of the scattering matrix that represents the amplifier is equal to zero. This definitions almost never occurs and the amplifiers are mostly bilateral, because both ports simultaneously influence each other.

2.5.5 Output matching network

The procedure on the configuration of a output MN is similar to the one performed on an input MN and the following expression is the one that best describes the considerations that one must take [24] :

$$\Gamma_{OUT} = S_{22} + \frac{S_{12} S_{21} \Gamma_S}{1 - S_{11} \Gamma_S} \tag{2.40}$$

It is possible to see the influence of Γ_S in Γ_{OUT}. If either this value or S_{12} are equal to zero the previous expression takes the form of equation 2.41 which is related to an unilateral amplifier.

$$\Gamma_{OUT} = S_{22} \tag{2.41}$$

2.6 LNA design

The design of a LNA must take into consideration three important parameters: gain, Noise Figure (NF) and stability. There must be a compromise taken by the designer so that all those parameters can meet the target goals.

2.6.1 Gain

When dealing with the design of a microwave amplifier, the power gain is the most relevant one among the other types that are implicit to it (voltage, current and power). The LNA as it has been mentioned on subsection 2.2.4 is the first electronic device to be reached by the signal after its capture by the antenna. It is important that the gain is of higher value so that it can be measured on the following stages after the LNA. There are three different types of gain associated to the microwave amplifier.

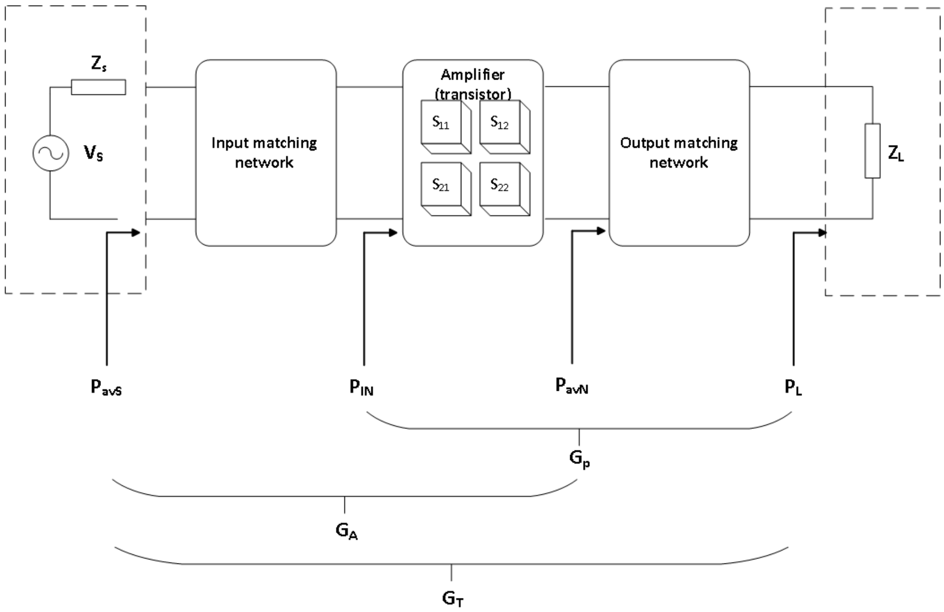

Figure 2.21: Different gains associated to the matching networks.

At figure 2.21 it is possible to observe the different power associated to each stage from the source to the load. It is possible to obtain the following expressions for each case [24]:

$$G_A = \frac{P_{avN}}{P_{avS}} = \frac{1-|\Gamma_S|^2}{|1-S_{11}\Gamma_S|^2}|S_{21}|^2\frac{1}{1-|\Gamma_{OUT}|^2} \tag{2.42}$$

$$G_P = \frac{P_L}{P_{IN}} = \frac{1}{|1-|\Gamma_{IN}|^2}|S_{21}|^2\frac{1-|\Gamma_L|^2}{|1-S_{22}\Gamma_L|^2} \tag{2.43}$$

$$G_T = \frac{P_L}{P_{avS}} = \frac{1-|\Gamma_S|^2}{|1-S_{11}\Gamma_S|^2}|S_{21}|^2\frac{1-|\Gamma_L|^2}{|1-\Gamma_{OUT}\Gamma_L|^2} \tag{2.44}$$

- G_A is the available power gain and it is the ratio between the power available from the network and the power available from the source. This result was provided by assuming that $\Gamma_L = \Gamma^*_{OUT}$ (maximum power transfer condition)
- G_P is the operating power gain and it is the ratio between the power delivered to the load and the power delivered to the input of the network. This result was provided by assuming that $\Gamma_S = \Gamma^*_{IN}$ (maximum power transfer condition)
- G_T is the transducer power gain and can be considered has the overall gain of the system since it is the ratio between the power delivered to the load and the power available from the source.

2.6.2 Noise Figure

The NF is one of the most important characteristics of a LNA. Having in mind what was discussed on subsection 2.2.5, the temperature of the antenna will be added to the temperature of the receiver. The major contributor for the last mentioned temperature is the LNA. So there is the need to decrease as much as possible the noise figure of the LNA. Being the first stage, this device must be carefully design to prevent the propagation of the noise through out the chain that leads to the final output. Reminding Table2.2 the letter F represents the noise factor. The Friis's law determines the noise's influence of all the components on the path of a signal.

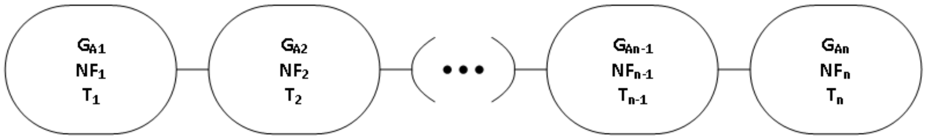

Figure 2.22: Chain of elements representing the path of the signal.

Taking as an example the figure 2.22, Friis determined the following expressions:

$$F_{total} = F_1 + \frac{F_2 - 1}{G_{A1}} + \frac{F_3 - 1}{G_{A1}G_{A2}} + ... + \frac{F_n - 1}{G_{A1}G_{A2}...G_{An-1}} \tag{2.45}$$

$$T_{total} = T_1 + \frac{T_2}{G_{A1}} + \frac{T_3}{G_{A1}G_{A2}} + ... + \frac{T_n - 1}{G_{A1}G_{A2}...G_{An-1}} \tag{2.46}$$

From both equations it is viable to conclude that the previous stages have an effect on the following ones. The biggest influence on the noise factor and on the noise temperature is given by the first stage (LNA). In expression 2.46 the contribution of F_1 and G_{A1} has a huge impact on the total result. It is due to that influence, that it is of high importance to design the LNA with a low level of noise and a high level of gain.

2.6.3 Stability

The stability factor is one of the most relevant constraints to the manufacturing of an amplifier. If certain conditions are not satisfied all the effort spent on the design of the other factors may be in vain. If the amplifier is not stable it will not perform as expected. Most likely it will oscillate instead of amplifying the signal as supposed. A transistor will oscillate if it has a negative real part either on the input or at the output port impedance. Physically a negative resistance does not exist, this is a mathematical concept that provides the means to understand the effect of the oscillation. A negative real resistance occurs when $|\Gamma_{IN}|>1$ or $|\Gamma_{OUT}|>1$. From equation 2.38 it is possible to see that Γ_{IN} is dependent of Γ_L. This means that Γ_L must also be inferior to one. In a similar way, from equation 2.40, it is possible to conclude that Γ_S must also be inferior to one. The stability can be measured with the aid of the s-parameters, the matching networks and values of the terminations (source and load). There are two situations that are possible to occur on an amplifier, it can be either unconditionally stable or potentially unstable. Summarizing, the conditions to assure that an amplifier is unconditionally stable are the following ones:

$$|\Gamma_{IN}| < 1 \quad \text{and} \quad |\Gamma_L| < 1 \tag{2.47a}$$

$$|\Gamma_{OUT}| < 1 \quad \text{and} \quad |\Gamma_S| < 1 \tag{2.47b}$$

Throughout the literature that studies this subject there are other conditions that can guarantee mathematically the stability of the amplifier. One of the most known conditions is the Rollet's stability factor (or K-factor) named after its author - John Rollet.

$$K = \frac{1 - |S_{11}|^2 - |S_{22}|^2 + \Delta^2}{2|S_{12}S_{21}|} > 1 \quad \text{with} \quad |\Delta| = |S_{11}S_{22} - S_{12}S_{21}| < 1 \tag{2.48}$$

The above conditions are considered necessary and sufficient to guarantee the unconditionally stability of an amplifier. Another way to measure the stability is with the μ stability test or geometric stability factor. This parameter has the advantages of using only one condition and it also provides a quantification of the stability. This means that a higher value of μ is equivalent to a more stable system.

$$\mu = \frac{1 - |S_{11}^2|}{|S_{22} - \Delta S_{11}^*| + |S_{12}S_{21}|} > 1 \quad \text{with} \quad |\Delta| = |S_{11}S_{22} - S_{12}S_{21}| \tag{2.49}$$

When performing the stability check (with any of the factors mentioned above) it should be specified a much higher range than the bandwidth of study. If the amplifier is unstable at a determined frequency it most likely oscillate. Even though the designer is careful there is still a chance of the stabilization of the amplifier fails, so there are some techniques that can be implemented after the circuit's manufacturing [36][24].

- Introduction of a series or shunt gate resistance, although this technique is not suitable for LNA design since it degrades the noise figure.
- Introduction of a shunt drain resistance . This technique is more suitable for a LNA but it can cause a decrease on the gain.
- Introduction of a feedback between the drain and the gate, this way there is a reduction of the negative resistance of the transistor and there is also a decrease on the gain at lower frequencies. But this technique is also not suitable for a LNA since it degrades the NF.
- Introduction of a short-circuit quarter-wave length line designed to eliminate the gain at higher frequencies than the bandwidth of study, eliminating this way a possible source of oscillation.

2.6.4 Bias circuit

One of the aspects that has not yet been considered is the bias circuit. This is also an important characteristic of the overall design of any type of RF circuit and has an important impact on the design of a LNA. The network bias is accomplished by introducing passive components into the circuit. As it has been mentioned before, those type of components introduce parasitic elements that one has been avoiding by using microstrip lines. On data sheets of RF transistor, the manufacturer provides the S-parameters and the noise parameters obtained with a certain set of conditions. One of those conditions (along with constant room temperature of 298 K) is the bias point that was used to obtain those results. As it has been mentioned in subsection 2.3.3 at table 2.4, there are three types of configurations for a FET. The Common-Drain configuration is best applied on the output stage of an amplifier due to its low Z_{out} and low gain. The Common-Gate has high voltage gain, but low power gain. Finally the Common-Source has medium voltage gain but most importantly a high power gain, that is more suitable for the design of a RF amplifier. This last configuration has also the particularity of inverting the signal of the input at the output.

So in resume, the manufacturer proceeds a series of tests on the transistor and provides the information of the polarization and its influence on the gain and on the NF. When making the design of the bias network, it must respect the specifications that are inherent to the transistor that is being used. The minimum current (I_{DS}) and the drain-source voltage (V_{DS} is equal to the V_D on a Common-Source) that are applied to the transistor for it to work has it should are also supplied by the manufacturer. These items are called the recommended bias conditions and their main goal is to set the transistor to its quiescent point.

The bias network must have the least impact has possible on the rest of a RF design, but unfortunately that is quite difficult to be obtained. So the preferred choice is to make it simple so its interference is as low as possible. The use of a resistance at the gate and at the drain after the voltage supply provides the necessary current to obtain the quiescent point of the transistor. A capacitor connected to the resistance and to the ground will serve as a low-pass filter.

RF Choke

A RF choke circuit is necessary so that the RF signal does not damage the voltage supply, but most importantly does not escape the path that was designed for it. There are some options to design this circuit, but the most suitable one for the frequency of interest in this case is by using a quarter wavelength transmission line associated with a radial stub. The concept behind this is the following: a quarter wavelength ($\frac{\lambda}{4}$) is responsible for putting at its output the dual of what was at its input. In other words if at the input there is a short-circuit (low RF impedance) then at its output there will be an open-circuit (high RF impedance), the same concept also happens on the reverse case. Connected to the $\frac{\lambda}{4}$ there is a radial stub that is mainly used to provide a low RF impedance (short-circuit). This component has great advantages compared to the normal stub, since it does not require other types of components (tee junctions) on the design. in figure 2.23 it is possible to see the layout that was explained previous which provides the circuit for RF choke [37].

2.6.5 Commercial LNA

Nowadays there are many manufactures that have developed commercial LNA that can be used for different applications and frequencies. At table 2.5 it is possible to see some of the LNAs available on the market and that are suitable for the frequency of study. Although most o them have a very high gain, there NF is not as favorable as intended for the use on radioastronomy. The LNA that provides the best result for this area is the `ALN1000-10-3010` of the `WENTEQ microwave company`.

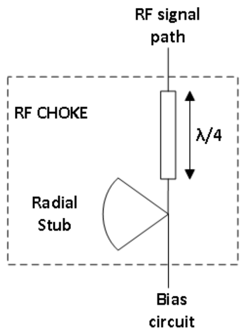

Figure 2.23: RF choke.

Designation	NF (dB)	Gain (dB)	Frequency range (GHz)
HD27028	1.8	17	7 - 14
ALN1000-10-3010	1.0	30	9.5 - 10.5
PE15A1004	3	38	12 - 18
PE15A1003	2.2	38	8 - 12
TGA2512	1.4	27	5 - 15
TGA2511	1.3	20	6 -14
WBA80130A	2.0	22	8 - 13

Table 2.5: Available LNAs on the market.

This LNA has NF of 1.0 dB and a gain of 30 dB, which is quite good, but its frequency range is very narrow when compared to the other transistors present at the table. There are also studies being conducted for the developing of new technologies using the transistors mHEMT that are appropriate for the use on the study of space [38]. Those technologies will be in the future responsible for better results on the construction of LNAs and the inherent decrease of its NF.

2.7 Concluding remarks

In this chapter there was a brief explanation of all the theoretical concepts that make the support and introduction for the design of a LNA at RF. A succinct introduction is made in order to understand the importance of the LNA and its NF on a radiometer receiver for radio astronomy. There was also a description of some relevant aspects that are important for the procedures that precedes the practical part of this assignment. Some of the contemporary available commercial LNAs are also displayed in this chapter, which will serve as comparison for the experimental results that will be attained posteriorly with this project.

Chapter 3

Simulations

3.1 Summary

In this chapter there is a presentation of the simulations that were taken to provide a support for the design of the circuit. Some relevant aspects, such as matching networks, noise figure gain and stability are mentioned and studied. The software used is MATLAB and ADS. At the annex it is provided the MATLAB code that supports the simulation.

3.2 MATLAB simulation

`MATLAB`[1] is a fundamental tool for the development of all sorts of work concerning complex and large amounts of calculations. The `RF Toolbox` provides a set of options to use on the construction of the MN and also the possibility of using S-parameter files provided by a manufacturer to simulate the transistor that is being tested. The bias circuit and also the RF Choke are quite difficult to simulate so they are not considered. The transistors that were tested for these simulations are on the list that follows:

Transistor	Description	NF (dB)	G_A (dB)
NE3511S02	GaAs Hetero Junction Field Effect Transistor (HJ-FET)	0.3	13.5
FHC40LG	GaAs HEMT	0.55	12
ATF-36077	GaAs pHEMT	0.5	12
MGF4953A	InGaAs HEMT	0.35	13.5
MGF4941AL	InGaAs HEMT	0.35	13.5

Table 3.1: Tested transistors.

All the transistors were chosen due to their qualities of a low NF and the possibility of being used at 10 GHz. They were also chosen due to their availability on the market and their physical characteristics. The values of G_A and NF were obtained by the manufacturers at a frequency test of 12 GHz and room temperature of 298 K.

[1] version used is 2013a

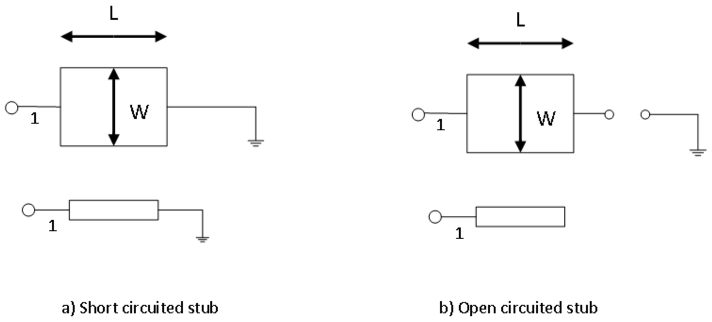

Figure 3.1: Symbols for the stubs.

3.2.1 Introduction

The performance required for a matching network becomes a challenge when it concerns the selections that needs to be taken. There are many types of matching networks. This simulation on MATLAB covers eight different types of matching network that are depict in figures 3.2 and 3.3. It does not intend to provide a complete description of a MN for a given transistor but instead its objective is to give a global idea of what choices should be taken, and what types of MN should be avoid. For a better understanding, in figure 3.1, there is a description of the symbols of the stubs that were used. This representation is similar to the one used on ADS by Agilent that was later used for the design of the LNA. The symbol for a short circuited stub is represented at figure 3.1a and the representation for the open circuited stub is at figure3.1b. The measure signed as L is the line's length and W stands for the line's width. This last dimension is related to the substrate (RT5880) that was used and since it is the same for each simulation the value for W is defined according to its specifications and is constant throughout the simulation. Figures 3.2 and 3.3 depicts the matching networks that were chosen to be used for both the simulations of the input and the output and are composed by stubs and/or lines all based in micro-strip technology. Figure 3.2 depicts the MNs which are composed by open-circuited stubs.In MN 1 and MN 2 the dimensions of l_1 and l_2 are the ones that change through each simulation. At MN 3 and MN 4, there is an added element that provides one more length (l_3) to be analyzed. Figure 3.3 depicts the MNs which are composed by short-circuited stubs. Similar to the MNs represented at figure 3.2, the first two MN have 2 lengths to be analyzed and the last two ones have 3 lengths for analysis. Some of the variables used on the `MATLAB` code are already defined. The source impedance (Z_S), the load impedance(Z_L) and the characteristic impedance of the line(Z_0) have all the value of 50 Ω. The specifications for the substrate are also defined in the function *matching_network.m* and were implemented with the following part of the `MATLAB`'s code:

```
e_r=2.2;
SigmaCond=5.96e7;
h_m=0.508e-3;
w_m=1.51e-3;
```

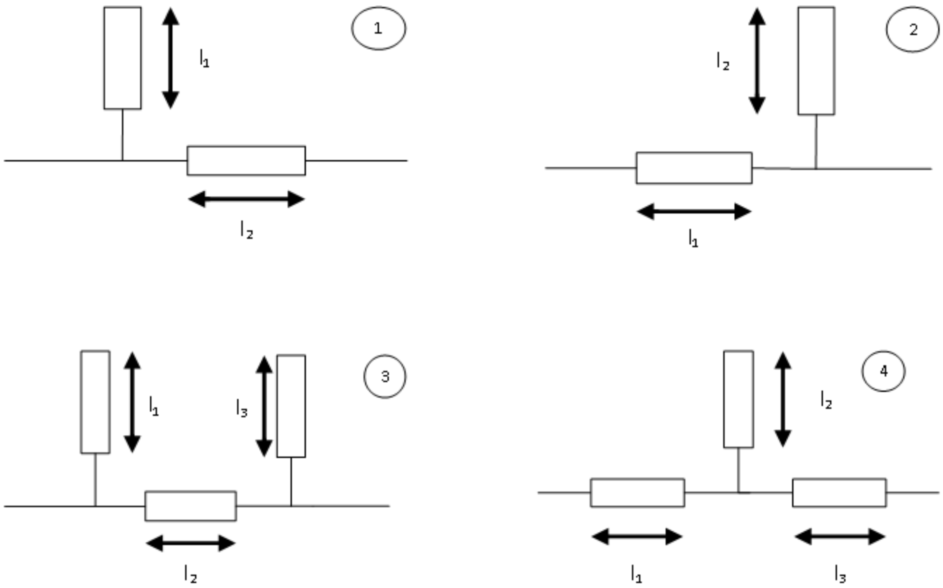

Figure 3.2: MN with open-circuited stubs.

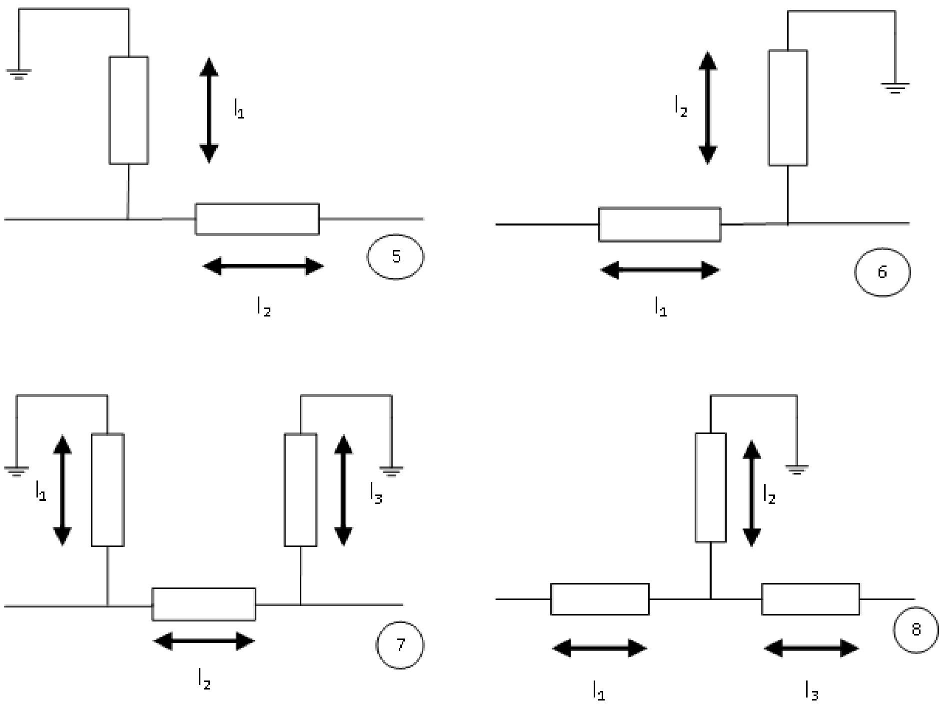

Figure 3.3: MN with short-circuited stubs.

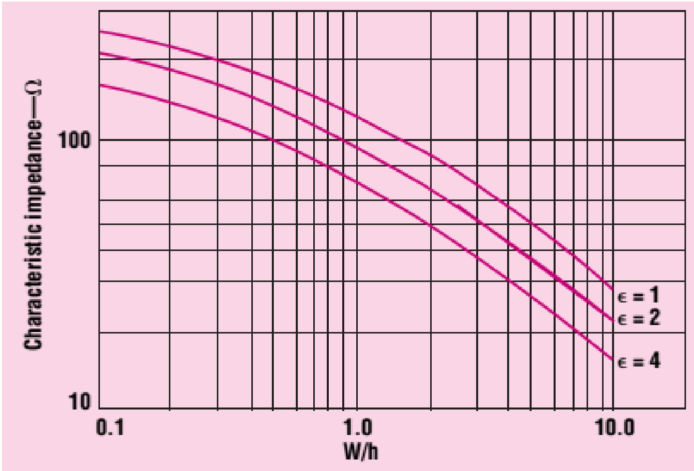

Figure 3.4: Characteristic impedance plotted for low dielectric constants.

```
t_m=35e-6;
l_tan=0.0009;
```

The value of W (width of the conductor) was calculated having in mind what was written on subsection 2.5.2. The substrate used is the RT5880 (`Rogers Corporation`), whose relative static permittivity (ε_r) is 2.2.

With the help of figure 3.4 [32] it is possible to see that for a Z_0 of 50 Ω the value to be expected for the ratio $\frac{W}{h}$ is higher than 2. So equation 2.37 satisfies that condition and provides the value for W. The final result for that parameter is 1.51 mm.

3.2.2 Functions

The microstrip lines were assembled with the help of the `RF Toolbox` (package `rfckt`). As an example, for the configuration of the MN 1 (figure 3.2), the part of the `MATLAB` code that performs that action is the following one:

```
stub1=rfckt.microstrip('Height',h_m,'LossTangent',l_tan,'
   EpsilonR',e_r,'Thickness',t_m,'SigmaCond',SigmaCond,'
   Width',w_m,'LineLength',l1,
'StubMode','Shunt','Termination','Open');
line2=rfckt.microstrip('Height',h_m,'LossTangent',l_tan,'
   EpsilonR',e_r,'Thickness',t_m,'SigmaCond',SigmaCond,'
   Width',w_m,'LineLength',l2);
MN=rfckt.cascade('ckts',{stub1,line2});
```

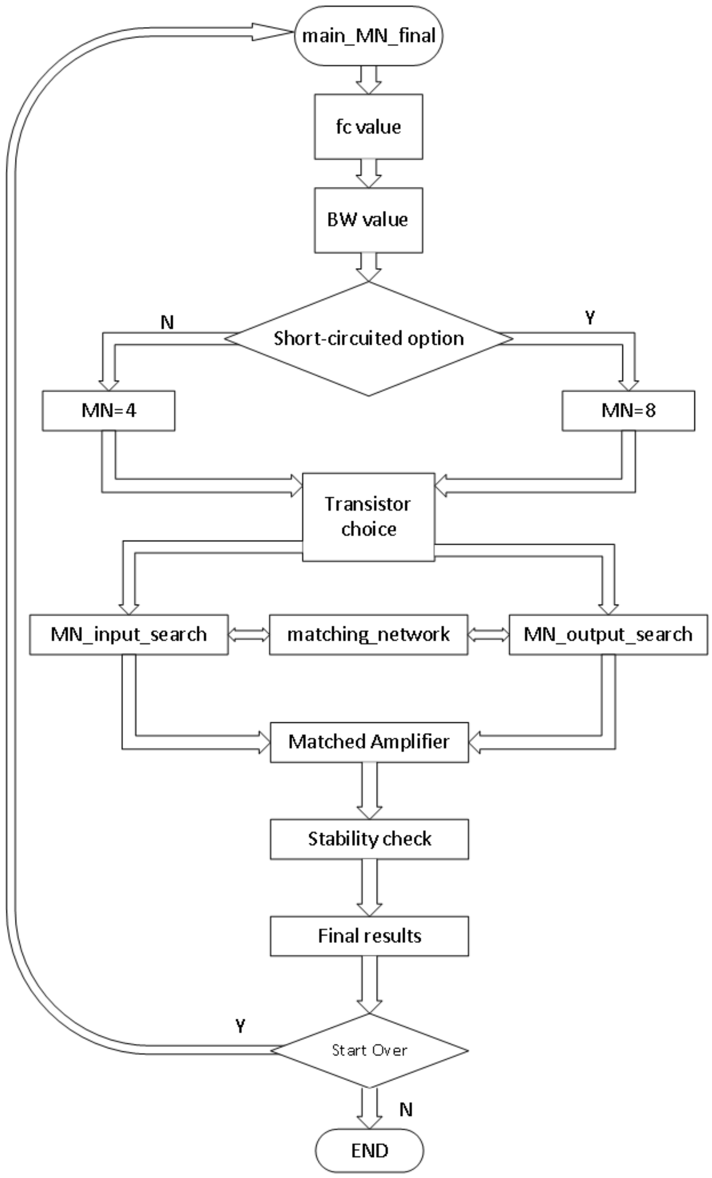

Figure 3.5: Flow chart of the simulation.

The flow chart depicted in figure 3.5 gives a description of what the program does. It starts by asking the user the value of the central frequency and the bandwidth that is intended to be used for the simulation. The central frequency and the bandwidth are used to specify a range of frequency values to be analyzed using the following `MATLAB` code:

```
Npts=41;
fLower=fc-(BW/2);
fHigher=fc+(BW/2);
freq=linspace(fLower,fHigher,Npts)
```

The next option that the user has is to choose between using or not short-circuited stubs. This option is required for mere academic study since this type of stubs are not recommended on practical implementations at high frequencies. A small menu

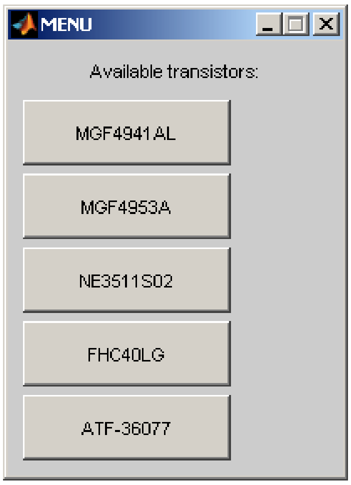

Figure 3.6: Menu that displays the available transistors.

appears (figure 3.6) that gives the user the option to choose a transistor from a list that is displayed on table 3.1. Their S-parameters' files are saved in the data base and they provide all the information necessary of the transistor. The next step of the program *main_MN_final.m* is the search of the best input and output MN for the specifications that were imposed by the user. The final matched amplifier is then assembled with the best input and output MN. A stability check is performed and the final results are displayed with graphics and images. At the end of the simulation, a text file is saved with the results, providing the best l_1, l_2 and l_3 and also the maximum NF and minimum gain that was obtained for each MN. The user has also the option of restarting the program and perform the simulation with different parameters.

3.2.3 Input matching network

Being a bilateral amplifier the output matching network has some effect on the NF but the biggest responsible for its decrease is in fact the input MN. For a better understanding of the construction of function MN_input_search, a brief review of concepts of chapter two is in order. Both input and output MN must satisfy the equation of the maximum power transfer (Equation 2.24). The output MN in this case is assumed to be perfectly matched. This means that $\Gamma_{out} = \Gamma_L^* = 0$. Having that in mind and making some substitutions on equation 2.38 the result is equation 2.39. Assembling all of the information mentioned it is possible to obtain the following expression:

$$\text{If} \quad \Gamma_S = \Gamma_{IN}^* = S_{11} \quad \text{then} \quad G_A = \frac{1 - |S_{11}|^2}{|1 - S_{11}S_{11}|^2}|S_{21}|^2 \tag{3.1}$$

Reminding both expressions 2.11 and 2.12, it is possible to see that the noise factor depends of a ratio between output and input temperatures (or powers) and of the G_A (expression 2.42). So this last one has an important impact on the noise factor. From expression 3.1 it is possible to conclude that the noise factor depends on S_{11}, which is

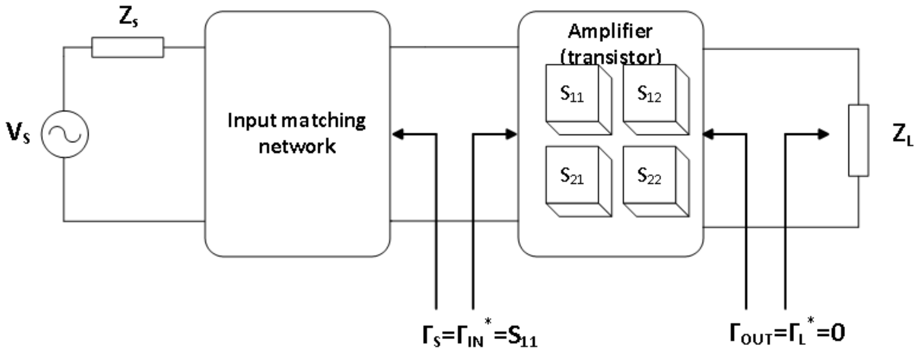

Figure 3.7: Input matching network.

the parameter that provides the accuracy of the input MN. This information proves that the input MN is responsible for the optimization of the NF.

Figure 3.7 served as reference to the development of the elements necessary to the construction of function *MN_input_search.m*. This last one uses a loop to calculate for each combination of l_1,l_2 and l_3 of a type of MN(figure 3.2 and 3.3) the NF associated with it. The NF itself is calculated by a specific function of `MATLAB RF Toolbox` . The range of values for l_1, l_2 and l_3 is from 0.1 mm to 7 mm with a step of 0.1 mm and the number of MN may be 4 or 8 (depending on the user input choice regarding the type of stubs). The function then makes a comparison between all the NF and chooses the set of l_1,l_2 and l_3 that optimizes each MN simulated. The last part of the function is the comparison between the NF associated to each MN and the choice of which is the one that has a best performance regarding the NF. Some of the code that implements this algorithm is the following:

```
Best_INMN=matching_network(best_i1,best_i2,best_i3,m);
Best_Matched_Amp=rfckt.cascade('ckts',{Best_INMN,Unm_Amp});
analyze(Best_Matched_Amp,freq,ZL,Zs,Z0);
Best_NF{m}=Best_Matched_Amp.AnalyzedResult.NF;
```

The first line makes the assembly of the best combination of l_1, l_2 and l_3 for a specific MN (variable 'm' represents each of the MN depicted at figures 3.2 and 3.3). The second line makes the assembly of the matched amplifier composed by the best input MN and the unmatched amplifier (which is configure with the S-parameter file provided by the manufacturer). The third and fourth line makes the calculation of the NF and stacks it in the variable 'Best_NF'.

The MN that provides the minimum NF is considered the best one. Take as an example the simulation of transistor MGF4953A, some of the results for the input MN are displayed at figures 3.8, 3.9, 3.10 and 3.11. The plots are saved in a file with the extension *".png"* and *".fig"*. This last one makes it possible for the user to edit with MATLAB and make better visualizations of the results.

In figure 3.8 it is possible to see that MN 1 has a very low NF when compared to the one of the MN 2 (Fig.3.9). Both figures are divided in to two parts. On the upper is the NF depending on the two lengths of the MN. In this color scheme the areas that are marked with red will be the worst combinations of lengths and that most likely

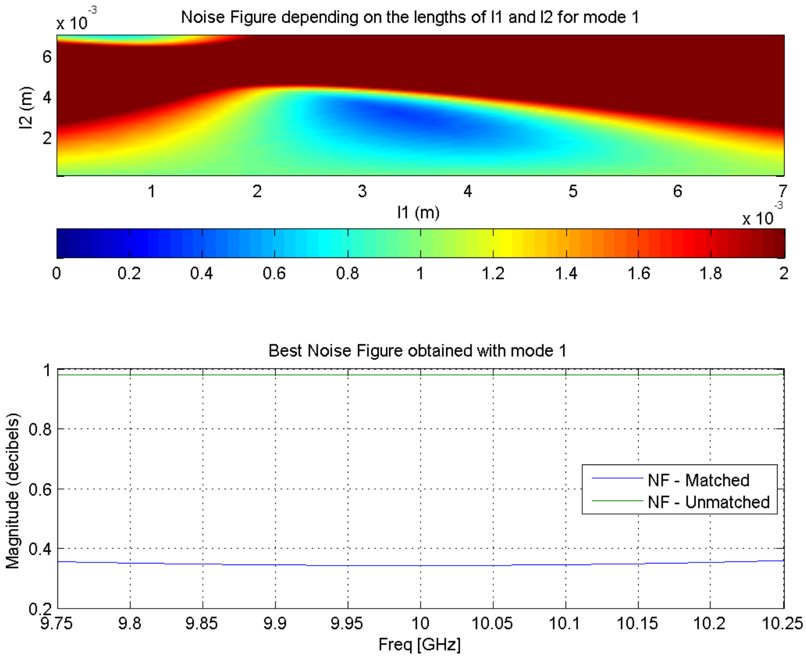

Figure 3.8: Noise figure for input MN 1.

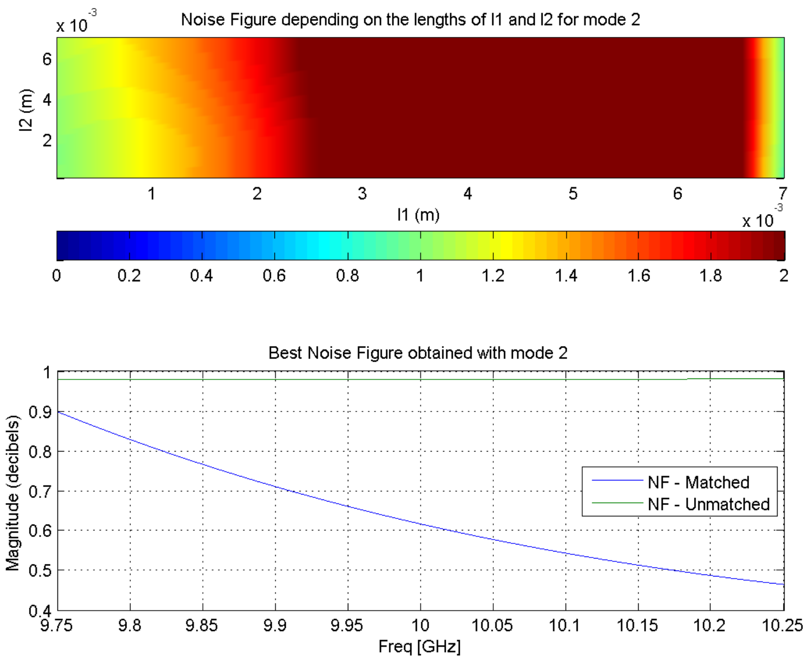

Figure 3.9: Noise figure for input MN 2.

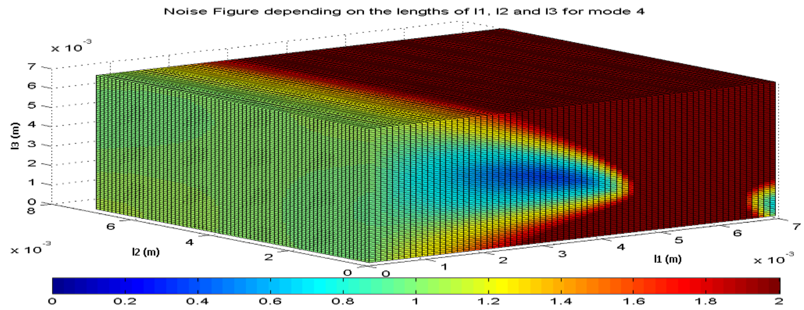

Figure 3.10: Noise figure for input MN 4.

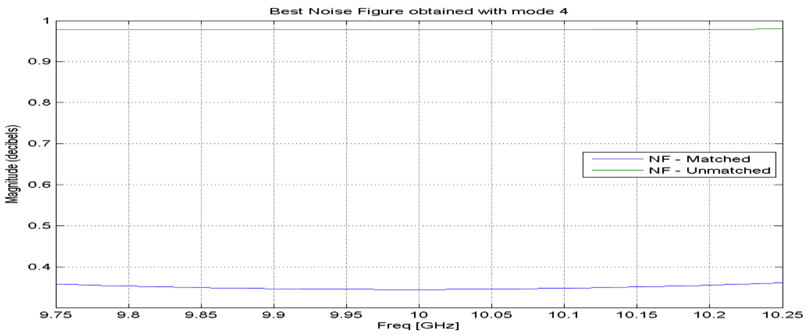

Figure 3.11: Noise figure for input MN 4.

will present bad values for the NF. On the lower part of the figure there is the NF depending on the specified central frequency and bandwidth (in this case f_c=10 GHz and BW=500 MHz). In this last figure it is shown both the plots of the unmatched and of the matched amplifier, so one can compare the results and take some conclusions.

Figure 3.10 shows a surface that has the value of the NF in function of three lengths (l_1,l_2 and l_3). Although it is harder to see the results in this figure, it is still possible to observe some of the places in the surface where the combination of the lengths provide the best and also the worst NF. Figure 3.11 depicts the plot of the MN 4 for the NF in function of the range of frequency that has been chosen. The results for this MN shows that the input MN is optimized and provides a good result for the NF.

3.2.4 Output matching network

The output MN is the most important issue to take in to account when dealing with the gain factor. Reminding some of the theoretical concepts introduced on subsection 2.6.1, there are three types of gain that can be calculated for a matched amplifier. Assuming that the input MN is perfectly matched, this means that $\Gamma_S = \Gamma_{IN}^* = 0$. Making substitutions of this conditions on equations 2.25, 2.42, 2.43 and 2.44 the following expressions take place:

$$\Gamma_{OUT} = S_{22} \tag{3.2}$$

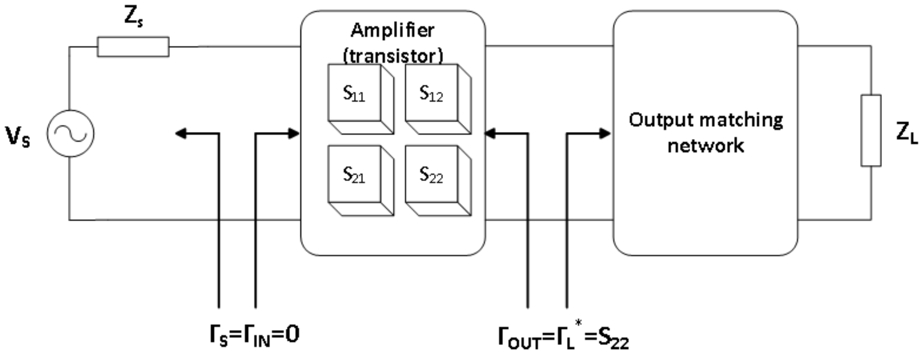

Figure 3.12: Output matching network.

$$G_A = \frac{|S_{21}|^2}{1-|S_{22}|^2} \tag{3.3}$$

$$G_P = |S_{21}|^2 \frac{1-|S_{22}^*|^2}{|1-S_{22}S_{22}^*|^2} \tag{3.4}$$

$$G_T = |S_{21}|^2 \frac{1-|S_{22}^*|^2}{|1-S_{22}S_{22}^*|^2} \tag{3.5}$$

It is possible to see that in this case $G_P = G_T$ and that all the expressions for the gains depends on S_{21} (forward transmission) and S_{22} (output reflection). This last parameter also provides an accuracy of the output MN what proves the importance of it on the gain factor of an amplifier. Just for curiosity if this parameter would be equal to zero (meaning that it would not exist reflections from the output), all the gains would be equal to each other $G_A = G_P = G_T = |S_{21}|^2$.

Figure 3.12 served as reference to the proceedings for developing function *MN_output_search.m*. Its algorithm is similar to the one used on *MN_input_search.m*, but the objective in this case is to find the MN that provides the best results concerning the gain factor. To do so the function makes a sweep through all the possible combinations of the lengths of the components for each MN. The gain that is calculated during this procedure is the G_T once again with the help of the `RF MATLAB Toolbox`.

The results that outcome of this function will complete the ones that were obtained previously with the function related with the input and constitute the matched amplifier.

At the upper part of figure 3.13 it is possible to see a long range of lengths' combination that have provided bad results for the gain (blue area) and at the lower part of the same figure it is possible to see that the value of the gain for the matched amplifier is slightly worst than the one for the unmatched.

At figure 3.14 it is possible to see that the results are much better than the ones obtained on the previous. This is the best case for the output MN of this transistor (although this is not true, because the best results surprising or not were obtained with the MN composed with short-circuited stubs, but since they are not easy to implement the choice falls on the MN 2 instead)

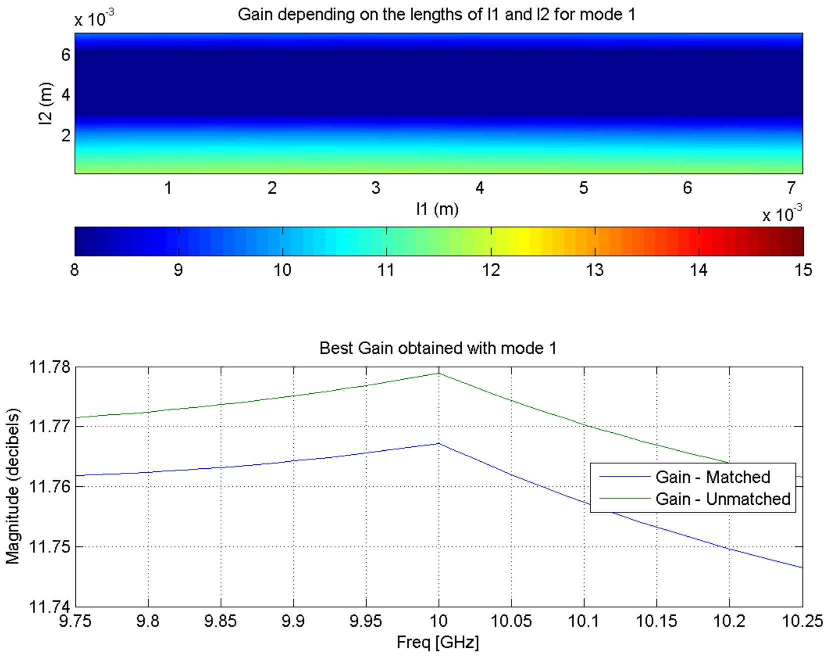

Figure 3.13: Gain for output MN 1.

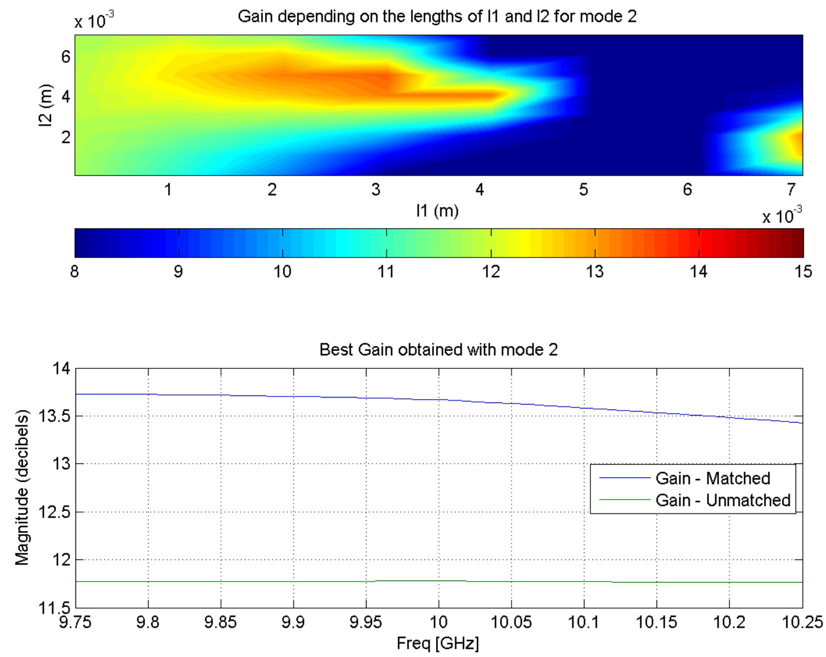

Figure 3.14: Gain for output MN 2.

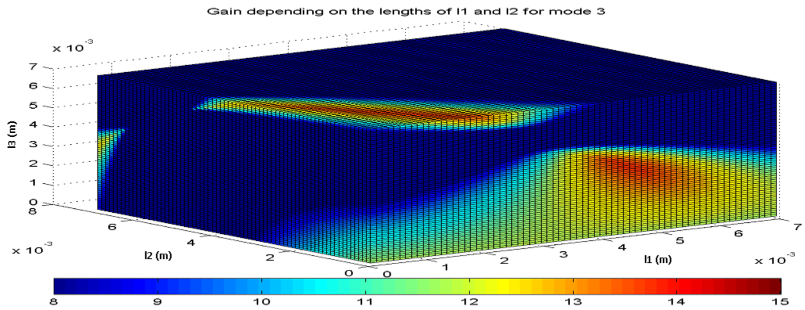

Figure 3.15: Gain for output MN 3.

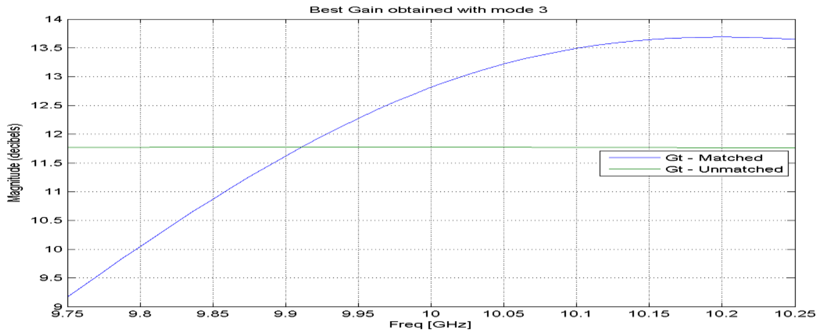

Figure 3.16: Gain for output MN 3.

At figures 3.15 and 3.16 it is possible to see a bad example of a choice for a MN of this transistor. The gain rises from approximately 9 dB till it gets to a constant value of approximately 13.5 dB. This occurrence may indicate some problems when making the tests with the final manufactured LNA, so it is better to avoided it.

3.2.5 Matched amplifier

After both input and output functions have terminated their search, the following step is the assemble of the matched amplifier. The part of the code that performs this action is the following:

```
Matched_Amp=rfckt.cascade('ckts',(inMn,Unm_Amp,outMn))
analyze(Matched_Amp,freq,ZL,ZS,Z0)
```

With inMn and outMn being the best input and output MN respectively for the transistor being study. The program then proceeds on making a final analysis of the matched amplifier to check the values of the NF and of the gain (G_T). The plots are then presented to the user containing the information regarding te overall NF and gain obtained for the final matched amplifier. Some of those results are portrayed at figures 3.17, 3.18, 3.19 and 3.20.

By analyzing figure 3.17 (corresponding to transistor MGF4953A) it is possible to see a flat line of the NF, equivalent to approximately 0.36 dB. This is a good result and it complies with the value provided by the manufacturer (table 3.1). Figure 3.18 is the

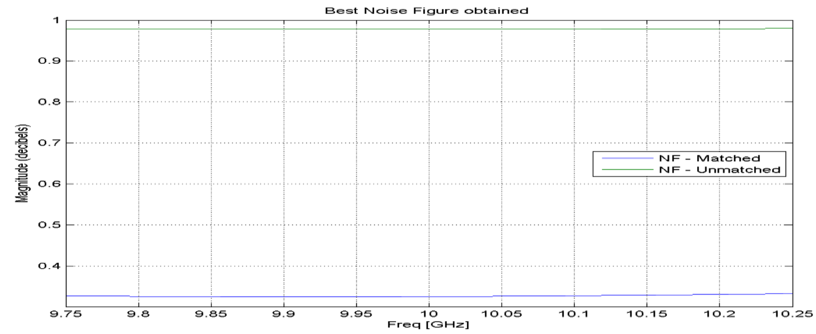

Figure 3.17: Best value of NF obtained with MGF4953A.

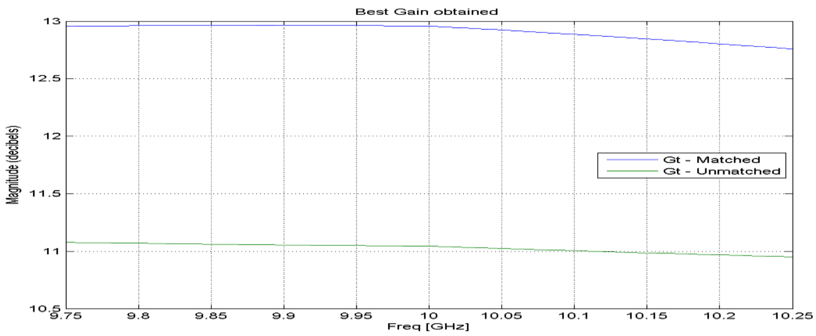

Figure 3.18: Best value of gain obtained with MGF4953A.

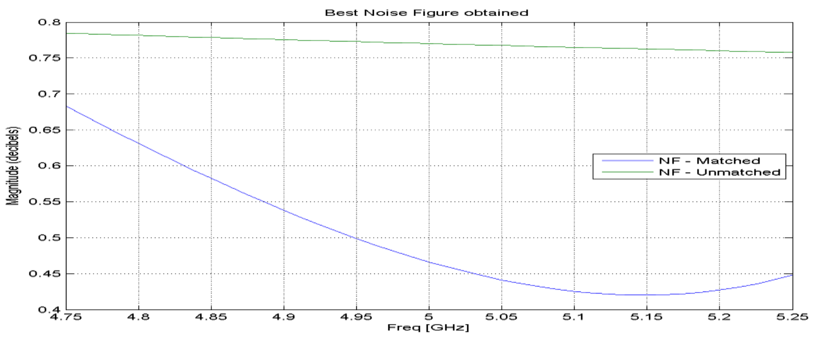

Figure 3.19: Best value of NF obtained with MGF4941AL.

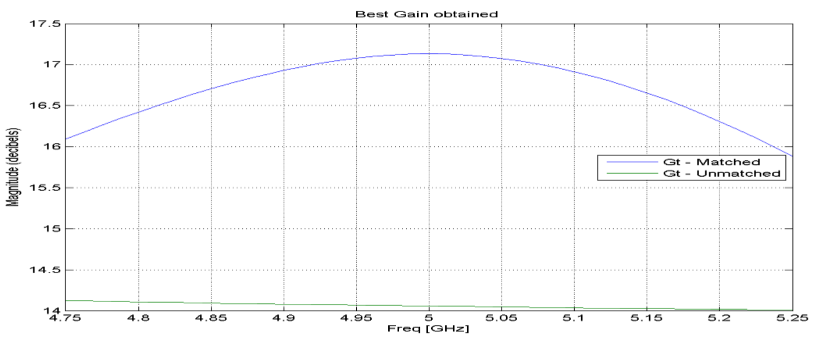

Figure 3.20: Best value of gain obtained with MGF4941AL.

representation of the plot for the gain, as it is possible to see this value is also quite good and it also complies with the value provided by the manufacturer. In conclusion, the transistor MGF4953A is the one that has the best performance for LNA design at 10 GHz. At figure 3.19 it is possible to see the results for the NF with transistor MGF4941AL. This value is not as good as the previous one, but still is the one that offered the best results at 5 GHz. Figure 3.20 is the representation of the plots for the gain. It is possible to see that for this case the gain is much higher and even though it does not have a constant value it is still also the best performance for the frequency of use. In conclusion, this transistor is the one most suitable for the LNA design at 5 GHz.

3.2.6 Stability check

An important issue that must be taken into consideration is the stability check. With the aid of the μ stability test (equation 2.49) it is possible to have some results that will provide conclusions about the quality of the matched amplifier and the transistor that was used. As it has been mentioned (subsection 2.6.3 the range of frequency should be much wider than the bandwidth for which the LNA is being optimized (although this is limited by the frequencies tested on the S-parameter file provided by the manufacturer). Some of the results that were obtained for each transistor are at figure 3.21.

As it is possible to see all the matched amplifiers show some issues regarding the stability. This was expected, since the simulation was not developed to optimize this factor, also there are still components missing on the MNs that will be added on the ADS simulation and that can modify the results for the stability.

3.2.7 Conclusions

At the end of the simulation, a figure of the equivalent MN that corresponds to the best input and output matching is displayed for the transistor that was being analyzed. Finally the results are saved on a text file. Those consists on the lengths of l_1, l_2 and l_3 (when applicable) that best suited each MN for the correspondent input and output configuration. The maximum overall NF and minimum overall gain that was obtained for each MN is present in that text file. And just for curiosity the time spent for the simulation is also displayed when using a less sophisticated computer. An example is provided at figure 3.22 which used the transistor MGF4953A. Some of the final results are presented at tables 3.2 and 3.3 that corresponds to the simulations for a f_c of 10 GHz and 5 GHz respectively. As a note, one must mentioned that for some transistors the input and output MN had better results with the use of short-circuited stubs. But since they are not easy to be reproduce at RF, their results will be neglected at these resumed tables.

From observing table 3.2 it is possible to see that the transistor that presents the best result for the NF is the NE3511S02 but its gain is relatively low when compared to others (it is also important to notice that by observing table 3.1, that this is a HJ-FET). The best result with a good compromise between the gain and the NF is obtained with transistor MGF4953A. At table 3.3 it is possible to observe that the

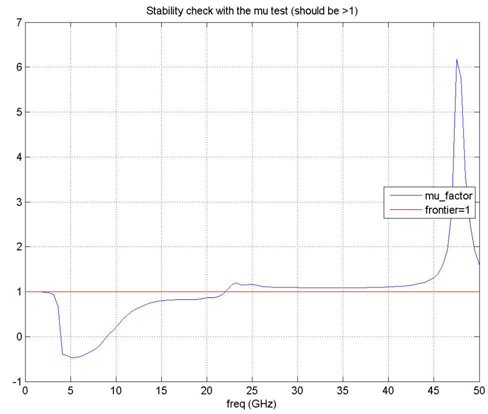

(a) Stability of the MGF4953A.

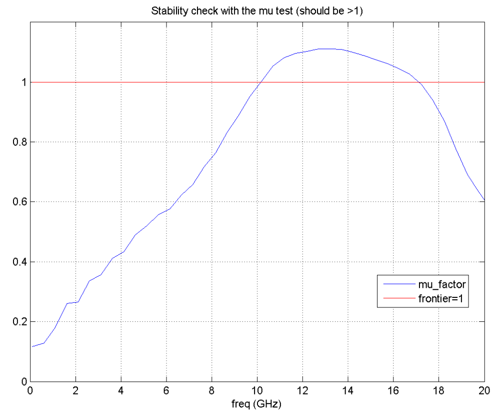

(b) Stability of the MGF4941AL.

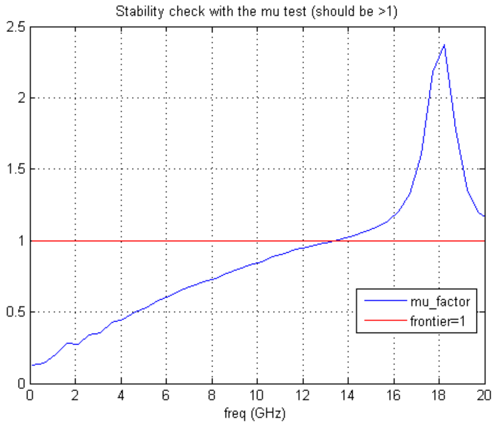

(c) Stability of the ATF-36077.

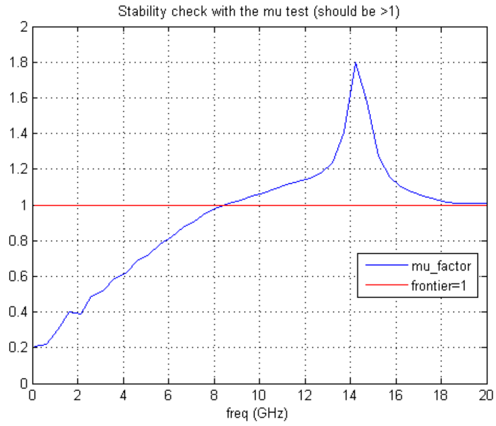

(d) Stability of the FHC40LG.

Figure 3.21: Plots for the stability.

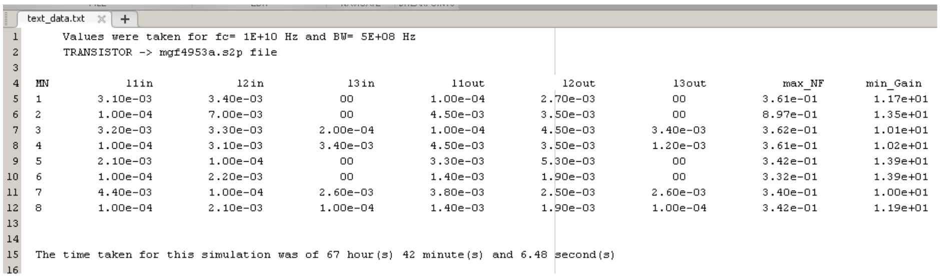

text_data.txt

Values were taken for fc= 1E+10 Hz and BW= 5E+08 Hz
TRANSISTOR -> mgf4953a.s2p file

MN	l1in	l2in	l3in	l1out	l2out	l3out	max_NF	min_Gain
1	3.10e-03	3.40e-03	00	1.00e-04	2.70e-03	00	3.61e-01	1.17e+01
2	1.00e-04	7.00e-03	00	4.50e-03	3.50e-03	00	8.97e-01	1.35e+01
3	3.20e-03	3.30e-03	2.00e-04	1.00e-04	4.50e-03	3.40e-03	3.62e-01	1.01e+01
4	1.00e-04	3.10e-03	3.40e-03	4.50e-03	3.50e-03	1.20e-03	3.61e-01	1.02e+01
5	2.10e-03	1.00e-04	00	3.30e-03	5.30e-03	00	3.42e-01	1.39e+01
6	1.00e-04	2.20e-03	00	1.40e-03	1.90e-03	00	3.32e-01	1.39e+01
7	4.40e-03	1.00e-04	2.60e-03	3.80e-03	2.50e-03	2.60e-03	3.40e-01	1.00e+01
8	1.00e-04	2.10e-03	1.00e-04	1.40e-03	1.90e-03	1.00e-04	3.42e-01	1.19e+01

The time taken for this simulation was of 67 hour(s) 42 minute(s) and 6.48 second(s)

Figure 3.22: Text file generated by the simulation.

Transistor	**Input MN**	**output MN**	**min NF (dB)**	**max G_T (dB)**
MGF4941AL	MN 1	MN 2	0.37	10.9
MGF4953A	MN 1	MN 2	0.36	13.4
NE3511S02	MN 4	MN 3	0.35	10.3
FHC40LG	MN 1	MN 1	0.55	10.4
ATF-36077	MN 4	MN 2	0.49	11.7

Table 3.2: Resume of the results obtained for each transistor at f_c of 10 GHz.

Transistor	Input MN	output MN	max NF (dB)	min G_T (dB)
MGF4941AL	MN 1	MN 2	0.75	14.6
MGF4953A	MN 3	MN 3	0.76	11.3
NE3511S02	MN 3	MN 3	0.78	11.8
FHC40LG	MN 1	MN 4	0.81	10.5
ATF-36077	MN 4	MN 2	0.78	10.7

Table 3.3: Resume of the results obtained for each transistor at f_c of 5 GHz.

results have decreased in quality for both important parameters. The transistor that presents the best values for these parameters is the MGF4941AL. The simulations performed by the `MATLAB` code, contributed to the following step that uses ADS.

3.3 ADS simulation

ADS was the elected program to perform the design of the LNA. This tool is of high importance for any designer of RF devices. Having the help of the MATLAB simulations and taking in consideration their availability it was possible to choose two transistors to work with. They are both from the same company (`Mitsubishi Electric`): MGF4941AL and MGF4953A.

3.3.1 Introduction

Working with ADS is quite helpful, since it provides a series of tools to differentiate almost all aspects of the circuit that is being designed. Unlike `MATLAB` this software is capable of reproducing both bias and RF choke circuits. It is also capable of simulating all the connections and junctions of the transmission lines and of the transistor.

The designer must take in to consideration not only the requirements of producing an efficient LNA but also the specifications on building the final Monolithic Microwave Integrated Circuit (MMIC). All minimal details must be carefully reproduced on the ADS simulation in order to guarantee accurate results that are as close as possible to the real ones. Most of the results of the simulations are for the transistor MGF4953A at a central frequency of 10 GHz and a BW of 500 MHz. Transistor MGF4941AL was simulated for a central frequency of 5 GHz and a BW of 500 MHz. This difference on the central frequency is for future comparison of the results of both transistors.

The simulation on ADS was divided into two groups. Using the S-parameter files and using the non-linear model of the transistor (both provided by the manufacturer).

3.3.2 S-parameter simulations

The first step of this procedure is to implement the best input MN that was obtained with the `MATLAB` simulation. The transistor is once again represented by the S-parameter file provided by the manufacturer. The lengths of the components are configured according with the results of the previous simulation. The next step is to make a first analysis by drawing the plots of the NF that is obtained at the output

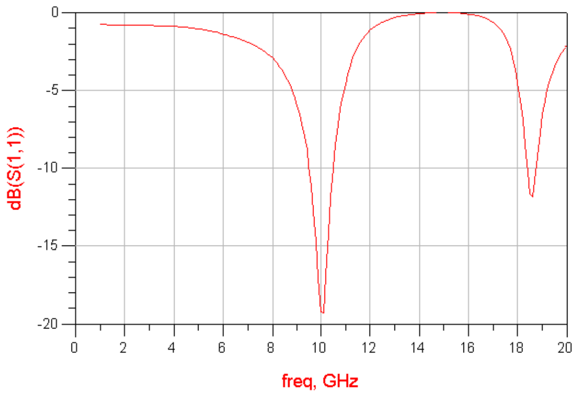

(a) Value of the S_{11}.

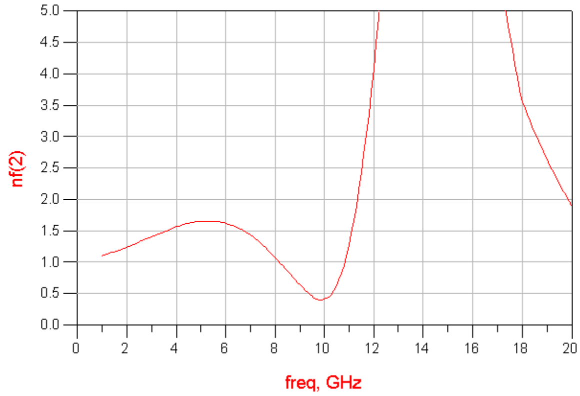

(b) Value of the noise figure.

Figure 3.23: Plots of S_{11} and of the noise figure.

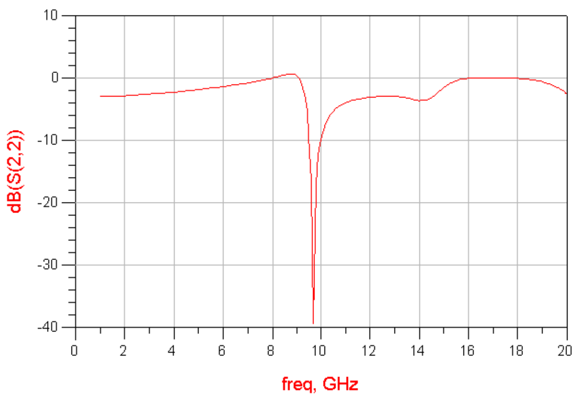

(a) Value of S_{22}.

(b) Value of the gain.

Figure 3.24: Plots of S_{22} and gain.

and of the $|S_{11}|$ in dB. This last value will provide a measure of the accuracy of the input MN, since the best possible result would be zero (no reflections at the input) its correspondent value in dB should be the most negative as possible at the frequency that is intended like is shown at figure 3.23a. Of course the value of the NF should also be has low as possible (figure 3.23b). With the help of the tunning tool it was possible to optimize the values of the lengths that would provide the desired results.

The next step is the implementation of the best output MN provided from the results of the `MATLAB` simulation. Similar to the input, the optimization of the gain and of the S_{22} parameter was made with the tuning tool. Like in the case of the S_{11} the value of S_{22} should be zero and the conversion to dB should get this value to be the most negative possible. At figure 3.24 it is possible to see the goals that are intended.

So by now the design of the circuit is the one depicted at figure 3.25. It is possible to see the terminals (corresponding to Z_S and Z_L) with the value of 50 Ω and the rest of the components that were mentioned. But this approach is very much incomplete, so the designer must consider some aspects relative to the real implementation of a MMIC. There should be a microstrip Line (MLIN) that simulates the connection that posteriorly will be made to the SubMiniature version A (SMA) connectors on both terminations (source and load). There should also be a reproduction of the connections that will be made to the transistor and that depends on its dimensions and package (provided by the manufacturer). The bias and RF choke circuit is missing. And finally two Direct Current (DC) block (appropriate capacitors) should also be added to the RF signal path to prevent the DC of flowing to the source and load which can cause serious damages and degradation of the NF.

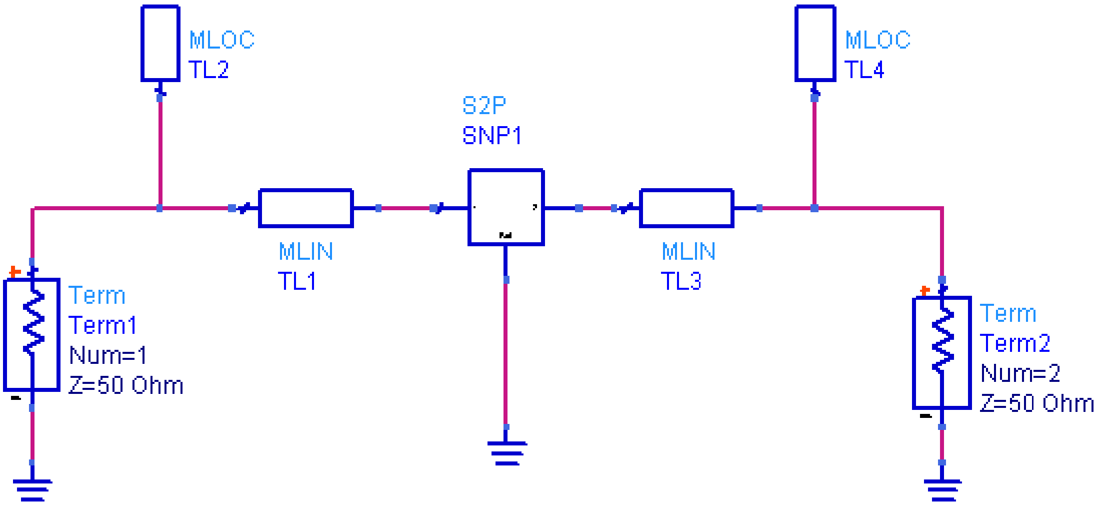

Figure 3.25: Preliminary circuit.

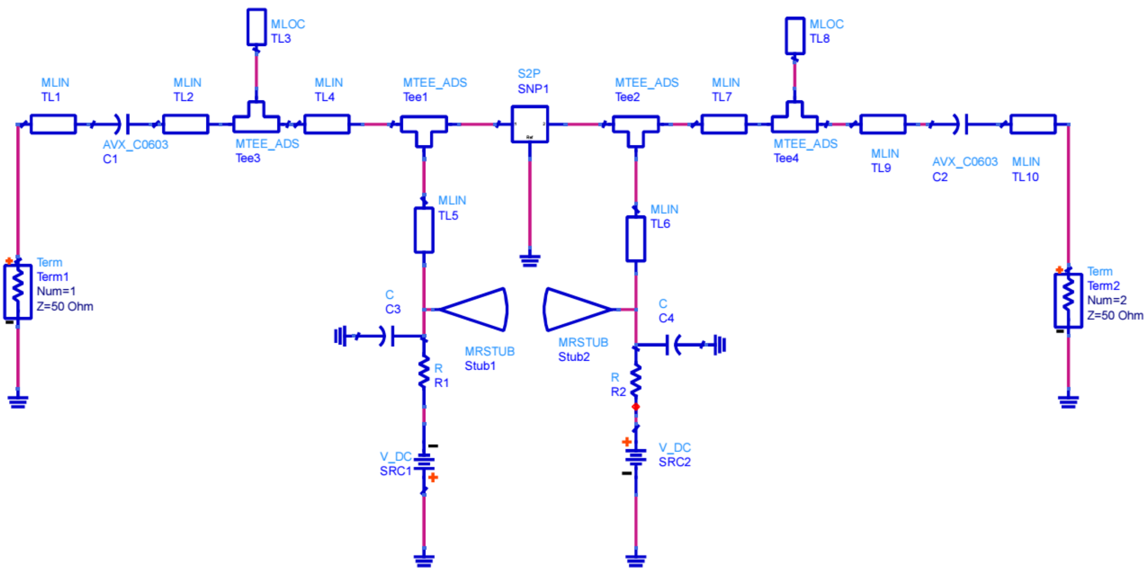

Figure 3.26: Final circuit.

The final circuit design is represented at figure 3.26. The bias circuit was configured having in mind the specifications provided by the manufacturer of the transistors. The quiescent point is obtained by having a I_{DS} of 10 mA and a V_{DS} of 2 V. The V_{GS}

should be considered in the interval of [-0.5, 0] V. As it is known, the capacitor at DC is considered to be an open circuit but at higher frequencies it is considered to be a short circuit. Although this is a very simplest approach, it is effective for explaining the rest. So for the bias circuit the only elements necessary are a resistance and a capacitor. Their values were calculated having in mind their availability and function on the circuit.

The RF choke (as it has been mentioned on subsection 2.6.4) is responsible for preventing the RF signal of diverging from the path that was designed for it and to avoid that it goes through the bias circuit. For the quarter wavelength line the values that are necessary to be calculated are its line's length and width. The value for the width (W) should be the lowest possible to provide a high impedance value (equation 2.33). So its value is dependent on the manufacturer that will produce the circuit. In this case the minimum possible value is 0.2 mm. The line's length is calculated using equation 2.26 and a tool of ADS that calculates the accurate value for ε_{eff} when provided with the frequency of use and the parameters of the substrate chosen. The value obtained with equation 2.26 is then divided by 4 and this is the final length value for the quarter wavelength. The parameters of the radial stub was obtained by simulation with ADS. By knowing that at the output of this component should be short circuit for RF and afterwards at the output of the quarter wavelength line there should be an open circuit. This means that at that point the gain should be the lowest possible.

The DC block formed by capacitors were obtained by researching for the ones that would provide a good result for a RF signal. After obtaining a package from a manufacturer that provided the models to use on ADS several simulations were so that a good choice of the capacitor can be made.

The Microstrip T-junction (MTEE)s were used so that they reproduce the connections between the stubs used and the lines which they are attached. They are also used to connect lines with different widths and finally the connections with the transistor.

The rest of the components were configured with the help of the tuning tool so that the best results for the important elements of the LNA could be obtained. Reminding that there has to be a compromise between the gain and NF.

The procedure that was explained previously is easily adapted for both the transistors and frequencies being used. The main difference resides on the dimensions and values of the components (DC capacitors, MLIN, Microstrip Line Open Circuit stub (MLOC), MTEE and radial stubs). At figure 3.27 it is possible to see the results for the NF and for the gain of the transistor MGF4953A. It is possible to see that at the central frequency and at the bandwidth chosen for this transistor, the NF is lower than 1 dB. The respective gain is above 13 dB, although its plots shows a peak of 16 dB between the f_H and f_L of the bandwidth. The representation of the simulations for the NF and for the gain of transistor MGF4941AL is depicted at figure 3.28. It is possible to see that the values for the NF are slightly better but now the central frequency of interest is half the one for the previous transistor.

A stability test was also performed, reminding equation 2.49, the value of mu should be higher than 1 so that the amplifier can be considered stable. At figure 3.29a it is possible to observe that the amplifier assembled with transistor MGF4941AL can be considered to be stable. As for the amplifier assembled with transistor MGF4953A

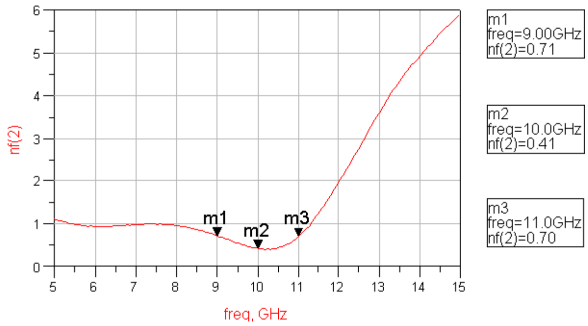

(a) Noise figure.

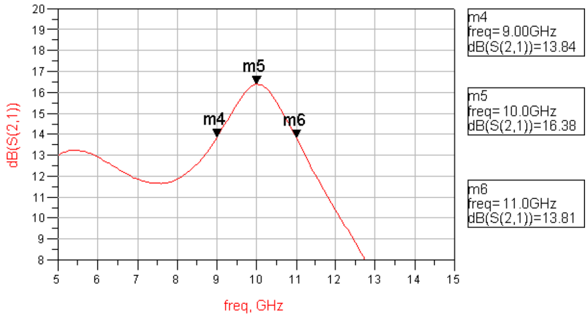

(b) Gain.

Figure 3.27: Results for the noise figure and gain of MGF4953A.

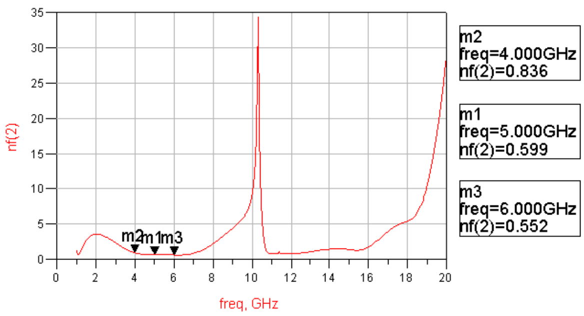

(a) Noise figure.

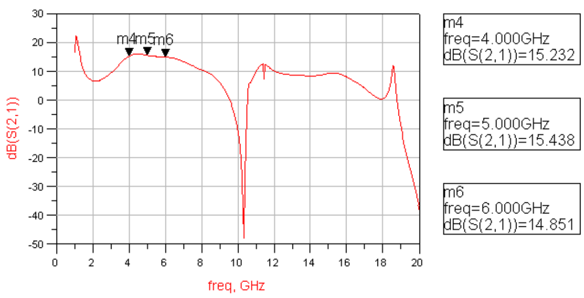

(b) Gain.

Figure 3.28: Results for the noise figure and gain of MGF4941AL.

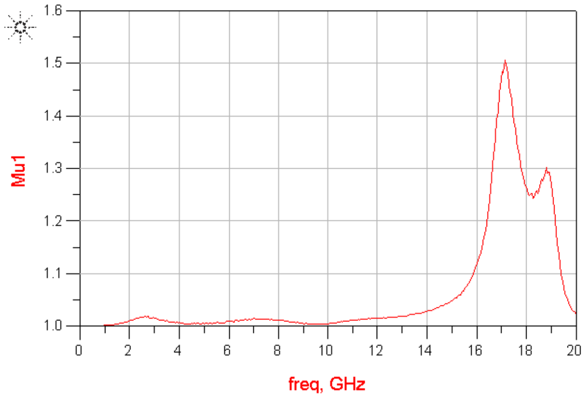

(a) Stability for MGF4941AL.

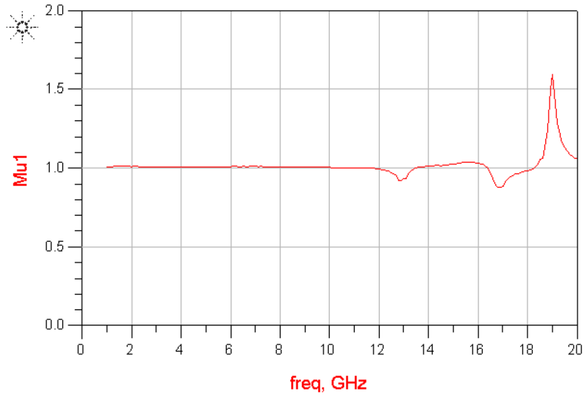

(b) Stability for MGF4953A.

Figure 3.29: Results for the stability.

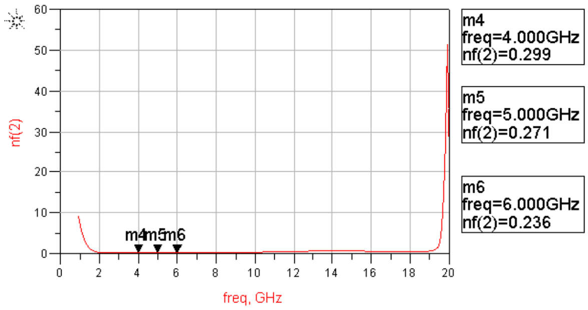

(a) Noise figure.

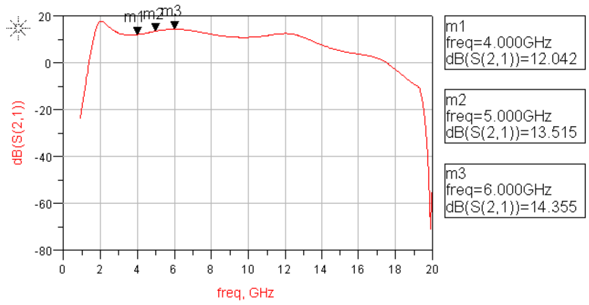

(b) Gain.

Figure 3.30: Results for the noise figure and gain of MGF4953A.

there are some frequencies at which the values of μ are slightly beneath the limit.

3.3.3 Non-linear model simulations

By working with two transistors of the same company (`Mitsubishi Electrics`) it was easier to obtain their non-linear models. The difference between these models and the study with the S-parameters file is that the non-linear models covers some aspects that the S-parameter does not. The design that was implemented is the same the only difference resides on the substitution of the S-parameter file of the transistor for the correspondent model. The dimensions of the components were also adjusted with the tunning tool of ADS.

3.3.4 Results

The results obtained for each transistor focus once again on the NF, gain and stability. Figure 3.30 depicts the plots for the results of transistor MGF4953A. It is possible to see that the value for the NF is much better but the gain has been slightly reduced (this is due to the compromise that the designer must take between both these parameters of a LNA). Figure 3.31 shows the plots of the results from the simulation

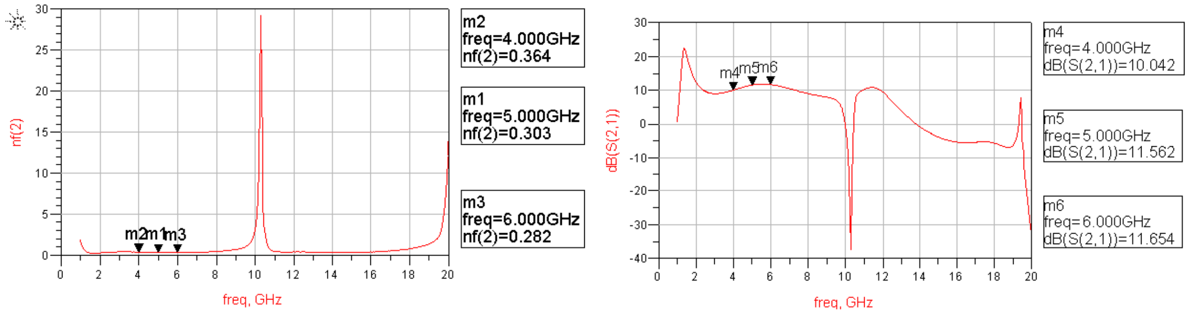

(a) Noise figure. (b) Gain.

Figure 3.31: Results for the noise figure and gain of MGF4941AL.

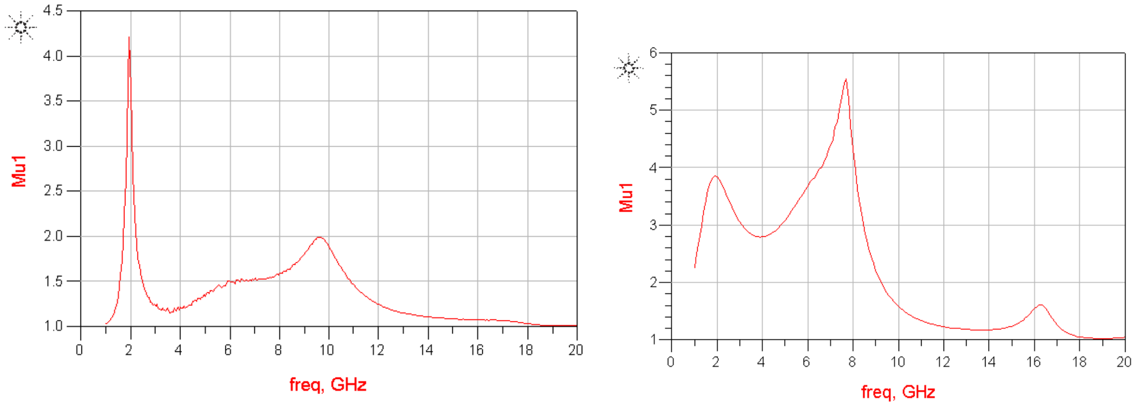

(a) Stability test for MGF4941AL. (b) Stability test for MGF4953A.

Figure 3.32: Results for the stability.

for transistor MGF4941AL. Once again it is possible to see the decrease of the value for the NF and also a decrease for the value of the gain.

By performing a μ stability test, it was possible to obtain the plots of these results that are illustrated at figure 3.32. The results for the stability test are much better than the ones obtained previously (figure 3.29).

3.3.5 Conclusion

The simulation with ADS was an extension of what was obtained with the `MATLAB` simulations. With the use of this program it was possible to obtain the values for each component that will be used on the final circuit. At table 3.4 it is possible to see the dimensions that will be used later when performing the layout. The table is divided in to two parts, one part for the dimensioning of the LNA that will use the transistor MGF4953A at 10 GHz and the other part is with the LNA that will be implemented with transistor MGF4941AL at 5 GHz. The component TL5 and TL6 are the quarter wavelength lines that compose the RF choke circuit. Their width is different (as it has been previously mentioned) and has the value of 0.2 mm. The other components have the width of 1.51 mm (measure relative to the substrate). The components that are missing on the table are the radial stubs dimensions. To characterize these elements,

		Dimension (mm)	
Component	**Designation**	**MGF4953A**	**MGF4941AL**
TL1	MLIN	2.38	0.72
TL2	MLIN	0.99	1.55
TL3	MLOC	1.30	1.14
TL4	MLIN	5.46	2.18
TL5	MLIN	5.5	11
TL6	MLIN	5.5	11
TL7	MLIN	3.34	3.55
TL8	MLOC	1.27	2.03
TL9	MLIN	1.27	1.14
TL10	MLIN	1.62	1.41

Table 3.4: Dimensioning of the circuits.

one must provide its radius and angle. For transistor MGF4953A their values are 3.26 mm and 90°respectively and for transistor MGF4941AL the radius is of 6.14 mm and the angle is also 90°.

3.4 Concluding remarks

The results obtained with both simulators were helpful on the choice of which transistors available on the market can have a reliable performance when implemented in to a LNA. The MATLAB simulation was useful to understand what types of matching networks can be utilized and which can ones should be avoided. It was also helpful to visualize a first glimpse of the NF and gain that the tested transistors can introduce on the LNA. The ADS simulation was crucial to visualize important aspects of the implementation of a LNA that were not covered with the (MATLAB simulation. It was also possible to make two types of simulations, one with the S-parameter file (similar to MATLAB simulation) and another one with the non-linear model of transistors. The results were promising and with the help of these powerful tools of simulation it was possible to advance for the next step of this project, that is the design of the layout and final construction of both LNA.

Chapter 4

Results

4.1 Summary

This chapter presents the achieved experimental results. There is a brief introduction to the layout, equipment and precautions that were taken into consideration.

4.2 Circuit layout

After the simulations performed in MATLAB and in ADS the next step was to design the layout of the circuit with the help of an other useful tool. While performing this layout the designer must respect the dimensions of the components that compose the final circuit. Figure 4.1 depicts the layout for the transistor MGF4941AL and figure 4.2 represents the layout for transistor MGF4953A. It is possible to see some differences between these two layouts. The first noticeable one is the length of the line that connects the radial stub to the main path of the circuit. This line has a quarter wavelength, so having in mind that the circuits are optimized for different frequencies and reminding equation 2.26 it is logical to assume that their lengths should also be different. The second noticeable difference is the size of the radial stub. For both cases its angle is of 90°, but the one depicted at figure 4.1 is much larger than the one used for transistor MGF4953A. This is due, once again, to the central frequency and the optimization of this component to perform an efficient RF choke. There are also differences regarding the connectors of the transistors and the dimensioning of the input and output MN. The gaps that are shown in both figures are for the connection of the capacitors and for the transistors. There are also two blocks at the lower part of both layouts at each left and right side. The two blocks on the left side correspond to the input voltage supply for the gate and the ground. The two blocks on the right side correspond to the input voltage supply to the drain and the ground.

This layout was then sent to a manufacturer with the right substrate (RT5880 in this case) to produce the test circuit. The construction of the circuit must take into consideration the layers that this project must have. Tracks are made over the substrate by following the instructions provided by the layout, this will be the top layer and also the signal layer. Another required layer is the one for the ground. To conclude the construction part, there is still missing the casing of the circuit made of brass. This is

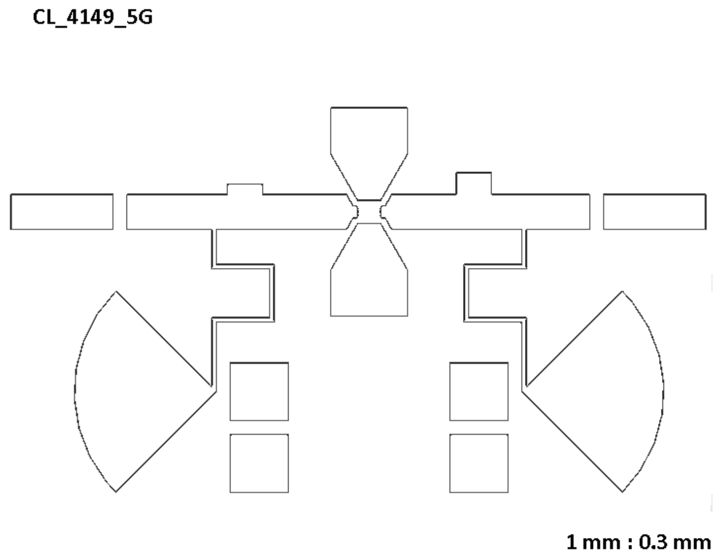

Figure 4.1: Layout for the MGF4941AL (f_c=5 GHz).

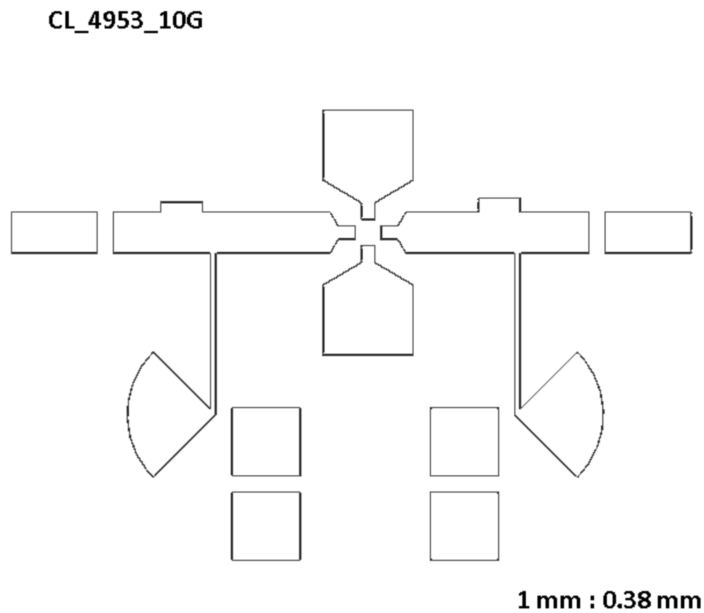

Figure 4.2: Layout for the MGF4953A (f_c=10 GHz).

Designation	Description	Range of use
HP8970A	Noise meter	10 to 1600 MHz
PL320QMD	DC Power supply (2 channels)	up to 32 V and 2 A
E8361C	PNA Network Analyser	10 MHz to 67 GHz
HP8593E	Spectrum Analyser	9 kHz to 26.5 GHz
SMR40	Signal Generator	10 MHz to 40 GHz

Table 4.1: Equipment used for experimental purposes.

necessary in order to guarantee an uniform ground plane and avoid some interferences when making the measurements.

4.3 Equipment

Table 4.1 shows the equipment that was required on this part of the project along with their specifications. The HP8970A was the device available for the measurement of the NF, it is also possible to measure the gain with this equipment. The PL320QMD is a dual channel power supply, this feature is necessary , since the circuit needs a positive (V_D) and a negative (V_G) voltage supply. The E8361C is the one responsible for providing a set of S-parameters for the circuit being studied. The HP8593E is a spectrum analyser, this equipment is responsible for providing the measure of the magnitude of the power's spectrum of an input signal throughout the range of frequency of this device (in this case 9 kHz to 26.5 GHz). The SMR40 is a signal generator that was used as a local oscillator (more about this device will be described in a following subsection). There were also some other special components that were used to help with the use of the noise meter. Such as an attenuator, a mixer, a commercial LNA and DC Blocks.

4.4 Stability test of the circuit

After the production of the PCB the next step was the circuit assemblage. Reminding the design depicted at figure 3.26, it is possible to see the components that are missing. After the complete assemblage of the circuit, the next step was to use the spectrum analyser to see the performance of the amplifiers. The first amplifier to be tested was the one with transistor MGF4953A optimized for 10 GHz. The analysis test showed that it was oscillating. The oscillation was at a frequency of approximately 18 GHz. Having the circuit already assembled, some solutions were advanced in order to mitigate this problem. The first solution that was tried, was the introduction of a shunt resistance on the drain, but this proved insufficient. The next solution was a little bit unorthodox, a thin slice of copper was introduced on the signal path and tested in different places with the objective of eliminating this oscillation. This procedure proved to be efficient since it was possible to cancel the peak at 18 GHz.

But still there were some problems with the circuit, when trying to use the network analyser to get the S-parameters, an error message was issued preventing this resource-

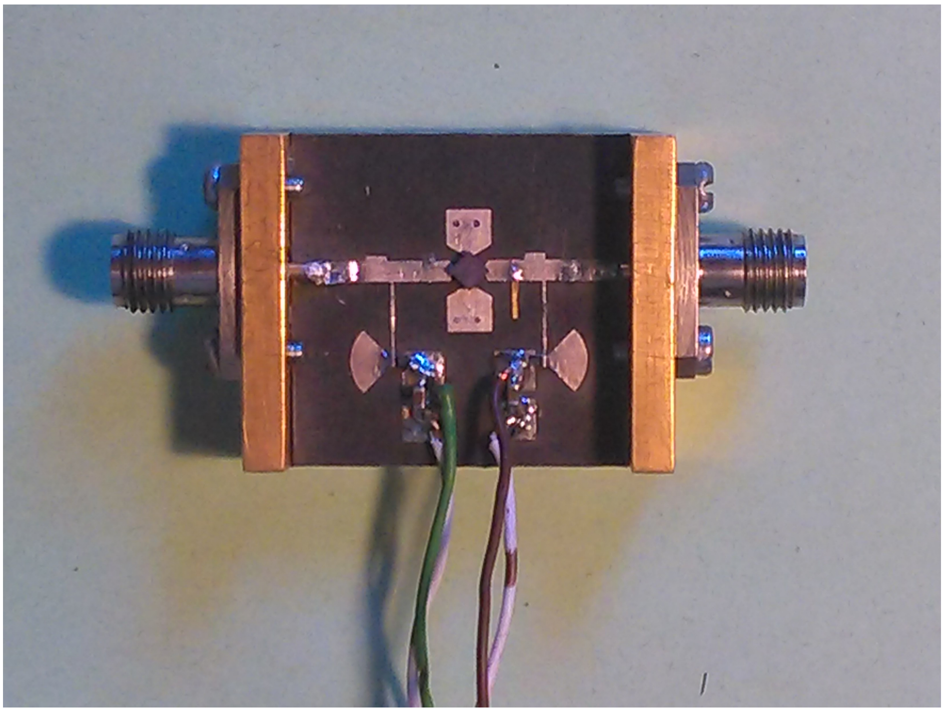

Figure 4.3: Final circuit for MGF4953A with alterations.

ful test. This error message had to do with oscillations that were still occurring. So the problem could be in other places. During the circuits' simulations, it were used capacitors with very low value for the DC blocks and with a very good behavior at RF. Unfortunately, when making the order for the manufacturer, these sort of capacitors were unavailable, thus compromising the design assumptions. The solution advanced was to remove those capacitors and cover the gap left by them on the signal path. After performing these procedures it was finally possible to obtain test results. The final circuit with the changes is displayed at figure 4.3

For the amplifier with the transistor MGF4941AL, the same problems occurred. So the same procedure that was performed for transistor MGF4953A took place. Figure 4.4 shows the final circuit of this amplifier with all the necessary modifications.

4.5 Measurement procedure

NF is the most important measure to make on a LNA (along with the gain). There are some concepts that should be revisited and new ones that must be added to fully understand the tests that were conducted in order to obtain the final results for this project.

Recalling equation 2.16, it is possible to see that V_{OUT} can be substituted by P_{OUT} if the units of the Boltzmann constant are changed from eVK^{-1} to JK^{-1} (table 1), thus obtaining equation 4.1. G is representing the gain of the radiometer receiver (or of the LNA as depicted at figure 2.9). This is the value of the noise power that will be read at the output of the system.

$$P_{OUT} = kBTG \tag{4.1}$$

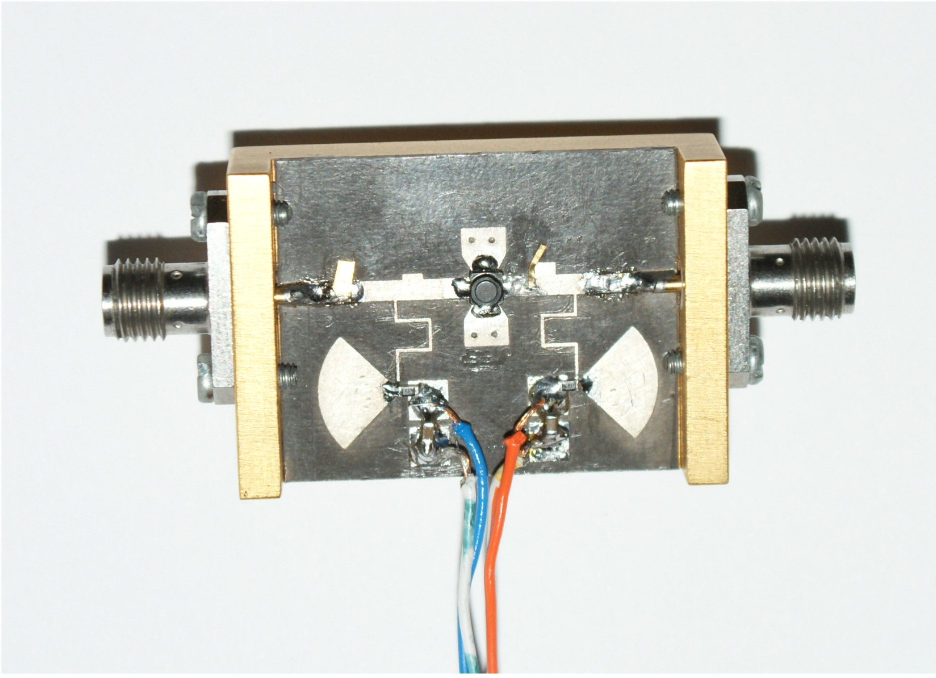

Figure 4.4: Final circuit for MGF4941AL with alterations.

4.5.1 Y Factor method

The Y factor method is known to be a useful technique on the measurement of the NF. The concept is quite simple, using equation 4.1 and making some substitutions it is possible to obtain the following expressions [27]:

$$\text{If} \quad T = T_{sys} + T_1 \quad \text{then} \quad P_1 = k(T_{sys} + T_1)BG \tag{4.2}$$

$$\text{If} \quad T = T_{sys} + T_2 \quad \text{then} \quad P_2 = k(T_{sys} + T_2)BG \tag{4.3}$$

The values of T_1 and T_2 are known in advance, so if one divides equation 4.2 by equation 4.3 the result is the following expression:

$$Y = \frac{P_1}{P_2} = \frac{T_{sys} + T_1}{T_{sys} + T_2} \tag{4.4}$$

Since the ratio between the two values of the power is known (Y) the only value that remains unknown is T_{sys}. And with that the following expression is obtained:

$$T_{sys} = \frac{T_1 - YT_2}{Y - 1} \tag{4.5}$$

Before adapting this theory to the practical case, one must first introduce another concept, the Excess Noise Ratio (ENR). The Y factor method comprehends the handling of a noise source that has a pre-calibrated ENR characterized by the following expressions:

$$ENR = \frac{{T_S}^{ON} - {T_S}^{OFF}}{T_0} \tag{4.6}$$

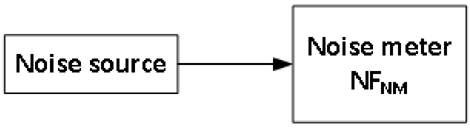

Figure 4.5: Simple chain of elements for a calibration.

$$ENR_{dB} = 10\log_{10}(ENR) \tag{4.7}$$

${T_S}^{ON}$ stands for the noise temperature of the noise source when its state is ON.
${T_S}^{OFF}$ stands for the noise temperature of the noise source when its sate is OFF.
T_0 stands for the standard room temperature which is equivalent to 290 K.

${T_S}^{OFF}$ is the physical temperature of the noise source and ${T_S}^{ON}$ is computed by the noise source with the help of expression 4.7.

$${T_S}^{ON} = 10^{ENR_{dB}/10}T_0 + {T_S}^{OFF} \tag{4.8}$$

There are also some precautions when making the measurements with the noise meter in order to avoid the introduction of error. One must avoid to expose the noise meter to fluorescent lights, nearby instruments and computers, cellular telephones and other types of communication devices while making the tests [39].

4.5.2 Calibration

Before making any type of measure with the noise meter it is important to calibrate the equipment. Before entering in to the details of this procedure, one must first understand the implementation of the Y factor method since it is a crucial tool for this part.

Figure 4.5 shows the noise source and the noise meter connected to each other. What this device does is setting the state of the noise source ON and OFF periodically and with this makes various measures of Y_{NM} to obtain a mean value of it that is more reliable to use. Expression 4.9 serves as reference for the calculation of this value and equation 4.10 completes it.

$$Y_{NM} = \frac{{P_{NM}}^{ON}}{{P_{NM}}^{OFF}} = \frac{{T_S}^{ON} + T_{NM}}{{T_S}^{OFF} + T_{NM}} \tag{4.9}$$

$$T_{NM} = \frac{{T_S}^{ON} - Y_{NM}{T_S}^{OFF}}{Y_{NM} - 1} \tag{4.10}$$

${P_{NM}}^{ON}$ is the value of the noise power generated by the noise meter when the noise source is ON
${P_{NM}}^{OFF}$ is the value of the noise power generated by the noise meter when the noise source is OFF
T_{NM} is the equivalent noise temperature of the noise meter

After obtaining all the previous values, the noise meter stores them and assigns for

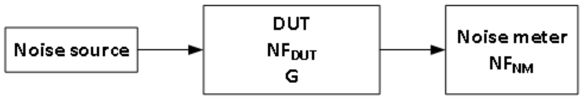

Figure 4.6: Simple chain of elements for a calibration.

the NF and gain the value of 0 dB that are then displayed for the user. These values are of high importance for the next step.

Figure 4.6 displays the introduction of the Device Under Test (DUT) on the chain of elements that was displayed at figure 4.5. The process used previously is then repeated and equations 4.11 and 4.12 serve as support for the calculations.

$$Y_{DUT+NM} = \frac{P_{DUT+NM}{}^{ON}}{P_{DUT+NM}{}^{OFF}} = \frac{T_S{}^{ON} + T_{DUT+NM}}{T_S{}^{OFF} + T_{DUT+NM}} \tag{4.11}$$

$$T_{DUT+NM} = \frac{T_S{}^{ON} - Y_{DUT+NM} T_S{}^{OFF}}{Y_{DUT+NM} - 1} \tag{4.12}$$

$P_{DUT+NM}{}^{ON}$ is the value of the noise power generated by the DUT and noise meter when the noise source is ON.

$P_{DUT+NM}{}^{OFF}$ is the value of the noise power generated by the DUT and noise meter when the noise source is OFF.

T_{DUT+NM} is the value of the equivalent noise temperature generated by the DUT and noise meter.

After obtaining all of the mentioned values it is now possible to calculate the value of the gain of the DUT. Expression 4.13 is used by most noise meter instrument devices for the calculation of the gain.

$$G_{DUT} = \frac{P_{DUT+NM}{}^{ON} - P_{DUT+NM}{}^{OFF}}{P_{NM}{}^{ON} - P_{NM}{}^{OFF}} \tag{4.13}$$

Finally, it is now possible to calculate the value of the noise temperature of the DUT with the help of the Friis' law (equation 2.46) and the final result is computed with expression 4.14:

$$T_{DUT} = T_{DUT+NM} - \frac{T_{NM}}{G_{DUT}} \tag{4.14}$$

The noise meter makes the calculation of the NF with the use of expressions 2.14 and 2.13. This last value is then displayed for the user to see.

Figure 4.9 is the final set-up of the circuit that was used for the measurements. The calibration for this case must take into consideration all of the elements that are before and after the DUT. This procedure is necessary to prevent the wrongful measure of the gain and NF of the DUT by establishing a calibration plane. So as a resume, the procedure that the noise meter carries on to make the measurements is the following:

- Calculation of the values for $P_{NM}{}^{ON}$, $P_{NM}{}^{OFF}$, Y_{NM} and T_{NM}.
- Calibration of the noise meter by setting its NF and gain to 0 dB.

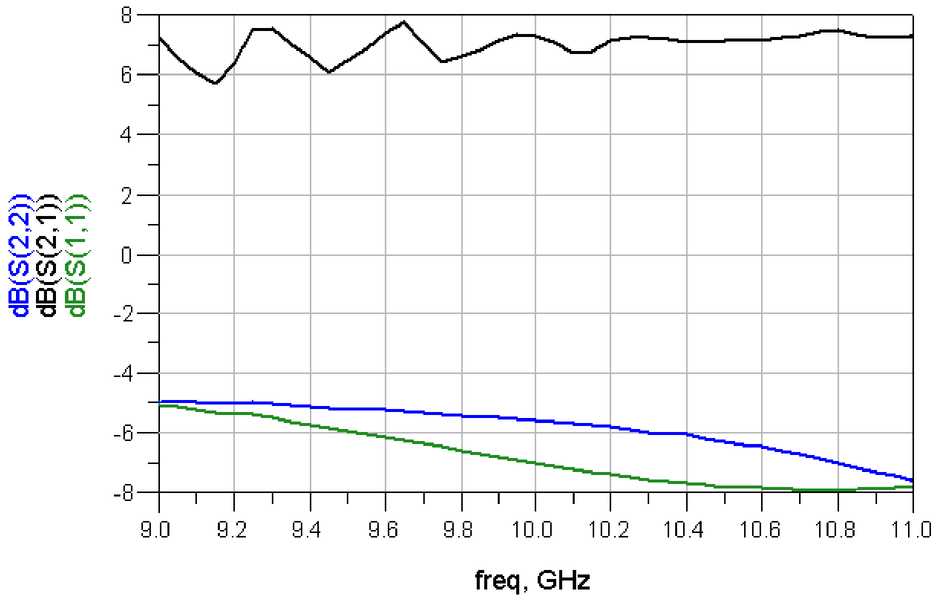

Figure 4.7: S-parameter file obtained for the LNA assembled with transistor MGF4953A.

- Introduction of all the components except the DUT in order to perform another calibration.
- Introduction of the DUT and obtainment of ${P_{DUT+NM}}^{ON}$, ${P_{DUT+NM}}^{OFF}$, Y_{DUT+NM} and T_{DUT+NM}.
- Calculation of G_{DUT}, T_{DUT} and finally the NF of the DUT that are both displayed on the noise meter.

4.6 Experimental results

With the help of the PNA Network Analyser it is possible to obtain the S-parameter files for the LNAs being tested. Those files where used on ADS in order to obtain the plots that are displayed in figures 4.7 and 4.8.

The NF and gain measurements was performed with the aid of a noise meter (HP8970A). Figure 4.9 represents the test circuit that was used for that purpose. For a better understanding of figure 4.9, a brief explanation is required. The DC blocks that appear are RF components that are connected to the SMA connector of the amplifier, their objective is to replace the capacitors that were previously removed due to issues with the stability. The pre-amplifier that appear in this figure is an expensive commercial LNA. Its goal is to increase the gain of the signal that is being read without introducing a high level of noise into the system. It is normally used when the noise meter has a high value of NF or when the DUT being analyzed has a low gain. The attenuator serves to weaken some of the possible mismatches that may occur on the test circuit and reduce reflections. The mixer is used to make a down conversion of the frequency. As it is possible to see at table 4.1, this noise meter has an operation

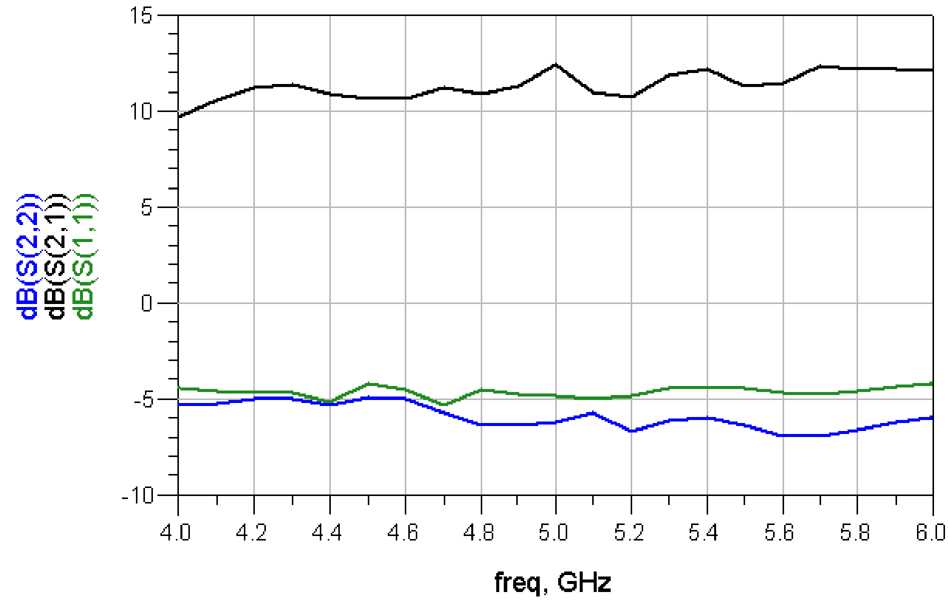

Figure 4.8: S-parameter file obtained for the LNA assembled with transistor MGF4941AL.

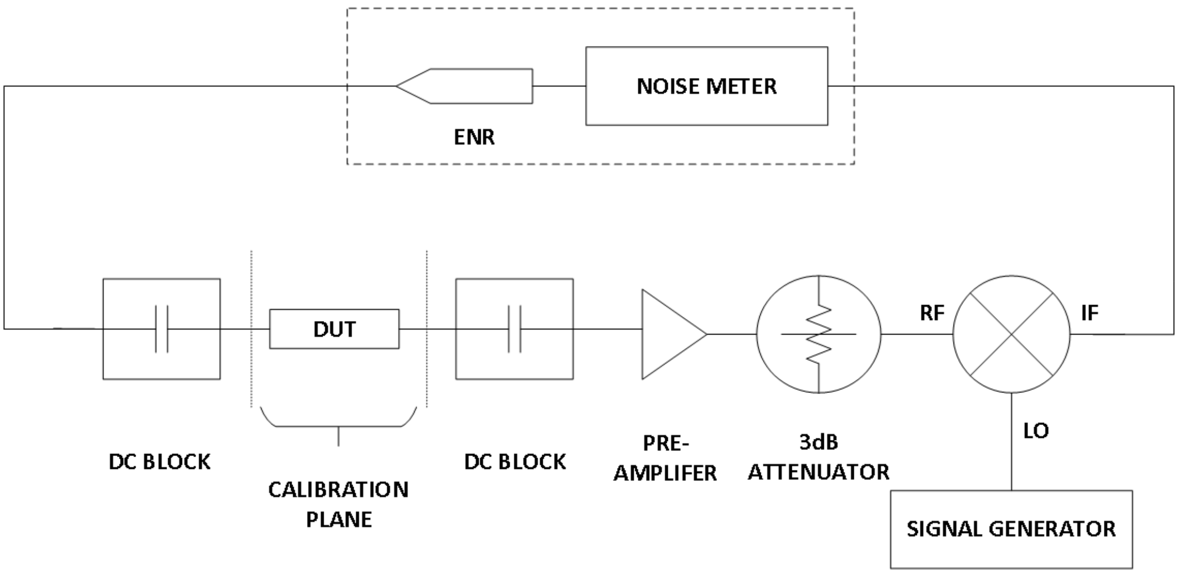

Figure 4.9: Set-up used on the noise meter.

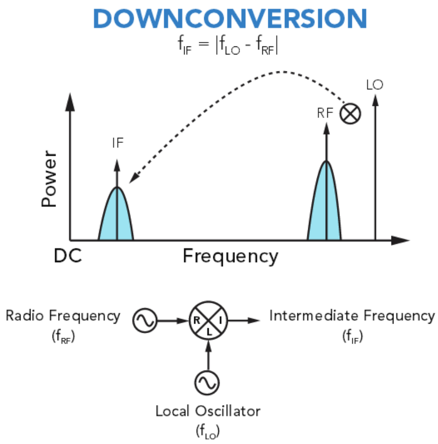

Figure 4.10: Down conversion [8].

LNA	NF (dB)	Gain (dB)	V_{DS} (V)	V_{GS} (V)	I_{DS} (mA)	f_c (GHz)
MGF4953A	1.59	7.59	2.2	-0.26	13	10
MGF4941AL	1.24	12.28	2.3	-0.31	11	5

Table 4.2: Obtained results for both LNAs.

range up to 1.6 GHz, but the lowest central frequency that was used is of 5 GHz. To overcome this problem it is necessary to use a RF mixer to perform a frequency down-conversion. This method is best described in figure 4.10 The frequency of the local oscillator is provided by a signal generator (SMR40). The method of down conversion is specified by the following expression:

$$f_{IF} = |f_{LO} - f_{RF}| \tag{4.15}$$

f_{IF} stands for Intermediate frequency
f_{LO} stands for Local Oscillator frequency
f_{RF} stands for radio frequency
The f_{IF} should be as low as possible so that the interaction with the noise meter has the best results. This has to do with the way that the instrument works, which implies a sweep through a very small bandwidth in order to calculate an average value of the NF.

After performing several bias tests in order to optimize both NF and gain, the best results obtained are described at table 4.2. By observing figures 4.7 and 4.8 it is possible to see that the values obtained for the gain with the PNA Network Analyser are in agreement with the ones obtained with the noise meter.

4.7 Concluding Remarks

After concluding all the experimental tests there are some issues that are pertinent to be discussed. The values for the S_{11} and S_{22} obtained from the network analyser

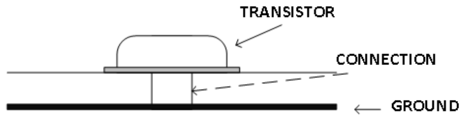

Figure 4.11: Impedance of the source.

show that the matching networks made for the amplifiers are not as perfect as one would intend, and that could be the cause for an increase on the value of the NF on both LNAs. The stability of both LNAs were of great challenge, and the introduction of external copper lines may also be a cause for the increase of the NF and the decrease of the gain on the LNA assembled with transistor MGF4953A. Another issue that should be discussed are the ADS simulations with the non-linear models. The results that outcome from these simulations showed a NF extremely low when compared to the experimental results, what leaves some doubts regarding the parameters associated with those models. As for the simulations with the S-parameters, they are more coherent. While the stability showed no problems with the non linear models (what proved to be wrong) the S-parameter simulation showed that there could be the possibility of occurring oscillations. Recalling figures 3.29a and 3.29b it was possible to see that with the μ stability test, that both LNAs were on the limit of stability at some frequencies. Even so, with some efforts, it was possible to obtain results on the experimental tests.

The most relevant issue that could be the cause for all the problems that occurred with the stability is the absence on the simulations of an impedance between the source of the transistor and the ground. From figure 3.26 it is possible to see that the simulations did not have in consideration the connections from the source to the ground that are possible to see at figure 4.11. The lack of an impedance that simulates this connection, introduces errors on the matching of the input network, what then leads to possible oscillations and an undesirable increase of the NF.

As a final remark one should make a comparison with the LNAs available on the market and that are displayed at table 2.5. From this table it is possible to see that the results concerning the NF are not as bad as the ones displayed here, while the gain is considerably low when making the comparison.

Chapter 5

Conclusions

5.1 Summary

In this chapter the conclusions are contemplated, also there is a proposal of ideas to a future work for someone that has interest in this challenging area. Some final remarks are made to terminate this academic work.

5.2 Conclusions

This dissertation was an attempt to introduce a new approach to the design of a LNA with cheaper transistors and new technologies (HEMT). The tasks that were followed were basically the same ones used in the design of any amplifier at RF. The difficulty was added with the need of designing a device with low noise level introduction, a proper gain and stable in a range that accommodates very high frequencies.

The results although somewhat not as desired as intended, were reassuring that the work was on the right track. Some faults and mistakes can be corrected and those were the ones that affected the final results of the circuit that was designed.

The first step of this hard work was the familiarity with the theoretical concepts that sustain the practical part. Research and investigation was made throughout papers and books of the subject. An overview of the existing LNA on the market was conducted to reassure a comparison with the ones developed.

The second step was the simulations of the future construction of the device. This part was of great help to understand some of the issues that can interfere with the final result. Both available softwares provided an interesting approach to the relevant aspects of the design, such as the matching networks and the considerations that must be taken to assure the maximum power transfer between the source and the load. The software also provided images and graphics that constituted a powerful tool to correct any inaccuracies that could damage the final work. Using the ADS it was possible to tune the parameters of the components that constituted the design. The only problem is that the values on simulation may not correspond to the ones that exist on the market.

The third step was the construction of the device. This was made with the help of technicians and professionals of the field. The LNA was manufactured and executed with the necessary requirements.

The fourth step was the testing of the device. This was the most delicate part because of the responsibility and the caution that one must take for not damaging neither the circuit or the equipment used for the tests. The operating point of the active part of the circuit (transistor) was of big importance since the voltage and the current admitted had an influence on the noise figure and on the gain. So a tune of the feed and a compromised between both gain and noise figure took place to assure the quality of the final response. Also there were some problems with the stability of the circuit that were of great challenge to solve and that can be responsible for the degradation of the final results.

5.3 Future work

Having in mind the results that were obtained, there are some aspects of this work that could be improved:

- The simulation created on `MATLAB` can be enhanced. This does not contemplate issues like the bias operating point of the transistor used neither other aspects that were latter introduced on the ADS simulation. Also other sets of matching networks can be added to improve the search.
- The transistors chosen for this work can also be updated, others are now available on the market that could add a better performance to the design of the LNA. And it would be a better approach to use transistors from different manufacturers.
- The use of the S-parameter files proved to be more accurate than the non-linear models, so a better approach would be to make a study concerning the non linear models and how they are obtained by the manufacturers.
- An interesting work would also be the construction of a radiometer receiver with all its components.
- It would also be interesting to conduct cryogenic tests in order to evaluate the performance of the LNA, considering that those are the environment conditions on the SKA project.

Bibliography

[1] National Radio Astronomy Observatory. Grote reber. http://www.nrao.edu/whatisra/hist_reber.shtml. Accessed: 2014-09-20.

[2] SKA Organisation/Swinburne Astronomy Productions. Ska artist's impression. https://www.skatelescope.org/multimedia/image/ska-night-dishes-pointing-towards-stars/. Accessed: 2014-09-20.

[3] National Aeronautics and Space Administration. Electromagnetic spectrum diagram. http://mynasadata.larc.nasa.gov/images/EM_Spectrum3-new.jpg. Accessed: 2014-09-20.

[4] Australian Telescope National Facility CSIRO. Askap's antenna. http://csirouniverseblog.com/2014/05/09/askap-spins-it-right-round-baby/. Accessed: 2014-09-20.

[5] Narelle Towie. Murchison widefield array (mwa) radio-telescope. http://www.theaustralian.com.au/news/m-murchison-radio-telescope-launched-iin-outback-wa/story-e6frg6n6-1226527575080. Acessed:2014-08-13.

[6] Luis Nero Alves. *Estudo e implementação de amplificadores em modo de corrente com grande produto ganho largura de banda.* PhD thesis, Universidade de Aveiro, 2008.

[7] By Fikret Altunkilic, Alan Miller, Vivian Tzanakos, and Michele Lewis. Designing Ultra Low Noise Amplifiers for Infrastructure Receiver Applications. pages 1–7, 2010.

[8] Ferenc Marki and Christopher Marki. Mixer basics primer: a tutorial for rf & microwave mixers. Technical report, Marki Microwave, 2010.

[9] Ieee standard letter designations for radar-frequency bands. *IEEE Std 521-2002 (Revision of IEEE Std 521-1984)*, pages 1–3, 2003.

[10] Jr. Jansky, C.M. The discovery and identification by karl guthe jansky of electromagnetic radiation of extraterrestrial origin in the radio spectrum. *Proceedings of the IRE*, 46(1):13–15, Jan 1958.

[11] IEEE Global History Network. Beginnings of radio astronomy. http://www.ieeeghn.org/wiki/index.php/Beginnings_of_radio_astronomy. Accessed: 2014-09-20.

[12] IEEE Global History Network. John d. kraus. http://www.ieeeghn.org/wiki/index.php/John_D._Kraus. Accessed: 2014-09-20.

[13] John D. Kraus and Alan T. Moffet. Radio astronomy. *American Journal of Physics*, 35(5):450–450, 1967.

[14] P.E. Dewdney, P.J. Hall, R.T. Schilizzi, and T.J.L.W. Lazio. The square kilometre array. *Proceedings of the IEEE*, 97(8):1482–1496, Aug 2009.

[15] Square Kilometre Array Project. Ska location. https://www.skatelescope.org/location/. Accessed: 2014-09-20.

[16] Donal A. Neamen. *Semiconductor Physics and Devices*. McGraw-Hill Higher-Education, 3rd edition, 2003.

[17] Peter Russer. *Electromagnetic, Microwave Circuits and Antenna Design for Communications Engineering*. ARTECH HOUSE, 2nd edition, 2006.

[18] Sophocles J. Orfanidis. *Electromagnetic Waves and Antennas*. 2014.

[19] Constatine A. Balanis. *Antenna Theory: Analysis and Design*. Wiley, 3rd edition, 2005.

[20] Max Planck. *The teory of heat radiation*. P. Blakiston's Son & Co., 1st edition, 1914.

[21] Eugene A. Sharkov. *Passive Microwave Remote Sensing of the Earth*. Springer-Praxis Books in Geophysical Sciences, 1st edition, 2003.

[22] Jack Smith. *Modern Commiunication Circuits*. McGraw-Hill International Editions, 1st edition, 1986.

[23] Frederick H. Raab Herbert L. Krauss, Charles W. Bostian. *Solid State Rado Engineering*. John Wiley & Sons, 1st edition, 1980.

[24] Guillermo Gonzalez. *Microwave Transistor Amplifiers: Analysis and Design*. Prentice-Hall Inc, 1st edition, 1984.

[25] A.A. Penzias. Measurement of cosmic microwave background radiation. *Microwave Theory and Techniques, IEEE Transactions on*, 16(9):608–611, Sep 1968.

[26] David Le Vine Niels Skou. *Microwave Radiometer Systems : Design and Analysis*. Artech House Inc, 2nd edition, 2006.

[27] C.W. McLeish G.Evans. *RF Radiometer Handbook*. Artech House Inc, 1st edition, 1977.

[28] Kenneth C. Smith Adel S. Sedra. *Microelectronic Circuits*. Oxford University Press,Inc, 5th edition, 2004.

[29] T. Mimura. The early history of the high electron mobility transistor (hemt). *Microwave Theory and Techniques, IEEE Transactions on*, 50(3):780–782, Mar 2002.

[30] Ralph S. Carson. *High-Frequency Amplifiers.* John Wiley & Sons, 1st edition, 1975.

[31] P. Eisler. Printed circuits: Some general principles and applications of the foil technique. *Radio Engineers, Journal of the British Institution of*, 13(11):523–538, November 1953.

[32] LG Maloratsky. Reviewing the basics of microstrip. *Microwaves RF*, 2000.

[33] E. Hammerstad and O. Jensen. Accurate models for microstrip computer-aided design. In *Microwave symposium Digest, 1980 IEEE MTT-S International*, pages 407–409, May 1980.

[34] H.A. Wheeler. Transmission-line properties of parallel strips separated by a dielectric sheet. *Microwave Theory and Techniques, IEEE Transactions on*, 13(2):172–185, Mar 1965.

[35] H.A. Wheeler. Reflection charts relating to impedance matching. *Microwave Theory and Techniques, IEEE Transactions on*, 32(9):1008–1021, Sep 1984.

[36] S .K. Leong. Stabilizing mosfet amplifiers. *MTT97 Convention in Denver*, 1997.

[37] Microwaves101. Quarter-wave tricks. `http://www.microwaves101.com/encyclopedias/quarter-wave-tricks`. Accessed: 2014-10-05.

[38] Axel Hülsmann, Arnulf Leuther, and Ingmar Kallfass. Advanced mHEMT technologies for space applications. *Proc. 20th Int. Symp. ...*, (April):20–22, 2009.

[39] Agilent Technologies. Noise figure measurement accuracy - the y- factor method. Technical report, 2014.

Appendices

Appendix A

MATLAB code

MATLAB functions

The following pages have the code that was created on MATLAB that supports the simulations that were presented on chapter 3. At table A.1 there is a presentation and a brief description of the functions that were developed for this work.

Function	**Description**
main_MN_final	Main function that supports all the others. Declaration of variables and code for the plots.
matching_network	Assembles the parameters of the MN for each set of l_1 and l_2 (and l_3 if it is the case).
MN_input_search	Calculates the NF for each MN and determines which one has the best performance.
MN_output_search	Calculates the Gain for each MN and determines which one has the best performance.
Stability_check	Calculates the μ stability test

Table A.1: Functions developed and their description

The first function is the *main_MN_final.m*, that is the main function that inter ligates all the others that follow.

main_MN_final

```
clear all
close all
clc
tic
global freq ZL Zs Z0 Unm_Amp aux Noise_Figure Gain Gain1 pathname Noise_Figure1 Best_N

Zs=50;              %source impedance
Z0=50;              %reference impedance
ZL=50;              %load impedance
```

```
aux=0.1e-3:1e-3:7.1e-3;     %auxiliar variable that defines the length size of l1 and l2


fc=0;                  %flag for the fc input procedure
BW=10;                  %flag for the bw input procedure

%% loop that provides a correct value for the fc
while(fc<=0 || isempty(fc))

    str1=('Input central frequency:   ');
    fc=input(str1);
    if (fc<=0)
        disp('Incorrect value for central frequency!')
    end
    if(isempty(fc))
        disp('no input value')
        fc=0;
    end
end
%%

%% loop that provides a correct value for the BW
while (BW<=10 || isempty(BW))
    str2=('Input bandwidth:   ');
    BW=input(str2);

    if (BW<=10)
        disp('Incorrect value for bandwidth')
    end
    if(isempty(BW))
        disp('no input value')
        BW=10;
    end

end
%%



%%  user input choice for using or not short circuited stubs
str3=('Would you like to use short circuited stubs? y/n   ');
reply=input(str3,'s');

if reply=='y'
    num_matching_networks=8;
else
    num_matching_networks=4;
end
%%

Noise_Figure=zeros(length(aux),length(aux),num_matching_networks);
%auxiliar variable that stores the different values for Noise Figure
Noise_Figure1=zeros(length(aux),length(aux),length(aux),num_matching_networks);
Gain=zeros(length(aux),length(aux),num_matching_networks);
%auxiliar variable that stores the different values for Gain
Gain1=zeros(length(aux),length(aux),length(aux),num_matching_networks);
```

```
Best_NF=cell(num_matching_networks,1);
Best_Gain=cell(num_matching_networks,1);

%%


%% menu that provides a choice for the available transistors
choice=menu2('  Available transistors:  ','MGF4941AL','MGF4953A','NE3511S02','FHC40LG

switch choice
    case 1
        s2pfile='mgf4941al.s2p';
        pathname='C:/Users/Calucas/Desktop/LNA/matlab_final/teste';
    case 2
        s2pfile='mgf4953a.s2p';
        pathname='C:/Users/calucas/Desktop/LNA/matlab_final/teste';
    case 3
        s2pfile='NE3511S02v2_2_18_2_10.s2p';
        pathname='C:/Users/calucas/Desktop/LNA/matlab_final/teste';
    case 4
        s2pfile='FHC40LG.s2p';
        pathname='C:/Users/calucas/Desktop/LNA/matlab_final/teste';
    case 5
        s2pfile='ATF-36077.s2p';
        pathname='C:/Users/calucas/Desktop/LNA/matlab_final/teste';
end
%%

%% analyze parameters
Npts=41;
fLower=fc-(BW/2);
fHigher=fc+(BW/2);
freq=linspace(fLower,fHigher,Npts);
%%

%% auxiliar variables for the stability (using mu factor)
freq1=linspace(100e6,50e9,100);
aux_mu=zeros(length(freq1),1);


%% analyzis of the unmatched amplifier using the s2p file of the transistor
Unm_Amp=read(rfckt.amplifier,s2pfile);
analyze(Unm_Amp,freq,ZL,Zs,Z0);
%%


%call of the function that provides the best INPUT matching network
[inMN,mIN,l1IN,l2IN,l3IN]=MN_input_search1(num_matching_networks);

%call of the function that provides the best OUTPUT matching netwotk
[outMN,mOUT,l1OUT,l2OUT,l3OUT]= MN_output_search1(num_matching_networks);


%% construction and analyzis of the matched amplifier
Matched_Amp = rfckt.cascade('ckts',{inMN,Unm_Amp,outMN });
analyze(Matched_Amp,freq1,ZL,Zs,Z0);
```

```
%%

%%  extraction of the s parameters matrix for the calculation of the stability
[sp, ~]=extract(Matched_Amp,'S_parameters');

for i=1:length(freq1)

    aux_mu(i)= s_p(sp(:,:,i));

end
%%
Matched_Amp = rfckt.cascade('ckts',{inMN,Unm_Amp,outMN });
analyze(Matched_Amp,freq,ZL,Zs,Z0);

%% plots of the results


figure;
plot(Matched_Amp,'NF')
hold all
plot(Unm_Amp,'NF')
hold off
legend('NF - Matched','NF - Unmatched','Location','East');
str2=sprintf('Best Noise Figure obtained ');
title(str2)


figfile = 'Best_NF';

saveas(gcf,[pathname,filesep,figfile],'png');
saveas(gcf,[pathname,filesep,figfile],'fig');


figure;
plot(Matched_Amp,'Gt')
hold all
plot(Unm_Amp,'Gt')
hold off
legend('Gt - Matched','Gt - Unmatched','Location','East');
str2=sprintf('Best Gain obtained ');
title(str2)

figfile = 'Best_Gain';

saveas(gcf,[pathname,filesep,figfile],'png');
saveas(gcf,[pathname,filesep,figfile],'fig');

aux_plot=ones(length(freq1),1);

figure
plot(freq1/1e9,aux_mu)
hold all
plot(freq1/1e9,aux_plot,'r')
hold off

xlabel('freq (GHz)')
```

```
legend('mu\_factor','frontier=1','Location','East');
grid on
title('Stability check with the mu test (should be >1)')


figfile = 'Stability';

saveas(gcf,[pathname,filesep,figfile],'png');
saveas(gcf,[pathname,filesep,figfile],'fig');
%%


%% display of the best MN for the input
figure('Name','Best model for the input matching network')

switch mIN
    case 1
        imshow('malha1.png')
    case 2
        imshow('malha2.png')
    case 3
        imshow('malha3.png')
    case 4
        imshow('malha4.png')
    case 5
        imshow('malha5.png')
    case 6
        imshow('malha6.png')
    case 7
        imshow('malha7.png')
    case 8
        imshow('malha8.png')

end

figfile = 'Best_inMN';

saveas(gcf,[pathname,filesep,figfile],'png');
saveas(gcf,[pathname,filesep,figfile],'fig');
%%

%% display of the best  MN for the output
figure('Name','Best model for the output matching network:  ')
switch mOUT
    case 1
        imshow('malha1.png')
    case 2
        imshow('malha2.png')
    case 3
        imshow('malha3.png')
    case 4
        imshow('malha4.png')
    case 5
        imshow('malha5.png')
    case 6
        imshow('malha6.png')
```

```
        case 7
            imshow('malha7.png')
        case 8
            imshow('malha8.png')

    end

    figfile = 'Best_outMN';

    saveas(gcf,[pathname,filesep,figfile],'png');
    saveas(gcf,[pathname,filesep,figfile],'fig');
    %%

    % write of a text file with the length, NF and Gain results for each MN
    clc
    format shortEng
    textfile='text_data.txt';
    fileID = fopen([pathname,filesep,textfile],'w');
    fprintf(fileID,'\tValues were taken for fc= %2.2G Hz and BW= %2.2G Hz\n\tTRANSISTOR -> %
    fprintf(fileID,'MN   \t\t l1in  \t\t\t l2in  \t\t\t l3in  \t\t\tl1out \t\t\tl2out \t\t\t


    for ia=1:num_matching_networks

        fprintf(fileID,'%d      \t %4.2d      \t %4.2d      \t %5.2d      \t %4.2d
    \t %4.2d      \t %5.2d      \t %4.2d      \t %4.2d\n' ,ia,l1IN(ia),l2IN(ia),l3IN(ia),l1O

    end
    %

    % % time taken for the simulation
    hours=floor(toc/3600);
    minutes=floor(rem(toc,3600)/60);
    seconds=rem(rem(toc,3600),60);

    fprintf(fileID,'\n\nThe time taken for this simulation was of %d hour(s) %d minute(s) an



    %% user option to start over the simulation with different parameters
    str5=('would you like to start over? y/n  ');

    reply1=input(str5,'s');

    if reply1=='y'
        main_MN_final1
    else
        return;
    end
```

The following scripts are a reproduction of the functions that search for the best input and output matching networks:

MN_input_search.m

```
%MN_input_search.m -> search for the best input matching network
%
%Usage: [bnf, bmi,best_l1,best_l2] = MN_input_search(MN_num )
%
%        ------------INPUT VARIABLES---------------
%MN_num -> number of matching networks in usage
%
%        ------------OUTPUT VARIABLES--------------
%bnf -> matching network with the best noise figure
%bmi -> best matching network's number
%best_l1 -> best length for l1
%best_l2 -> best length for l2
%best_l3 -> best length for l3


function [bnf, bmi,best_l1,best_l2,best_l3] =MN_input_search1(MN_num )

global aux  Noise_Figure Noise_Figure1 Zs Z0 ZL Unm_Amp freq pathname Best_NF

%auxiliar variable used on the Noise_figure calculation

mini_aux=2;

best_l1=zeros(MN_num,1);
best_l2=zeros(MN_num,1);
best_l3=zeros(MN_num,1);                        %only used on MN={3,4,7,8}



%auxiliar variable for the plots
[ll1,ll2,ll3]=meshgrid(aux,aux,aux);          %MN={3,4,7,8}
[l1,l2]=meshgrid(aux,aux);                     %MN={1,2,5,6}

for m=1:MN_num

    mini=2;
    mini1=2;

    for i1=1:length(aux)

        for i2=1:length(aux)

            if((m==3) || (m==4) || (m==7) || (m==8))

                for i3=1:length(aux)

                    INMN=matching_network(i1,i2,i3,m);
                    Matched_Amp = rfckt.cascade('ckts',{INMN,Unm_Amp});
                    analyze(Matched_Amp,freq,ZL,Zs,Z0);
                    aux2=Matched_Amp.AnalyzedResult.NF;
                    Noise_Figure1(i1,i2,i3,m)=max(aux2);

                    if (Noise_Figure1(i1,i2,i3,m)<mini1)
                        mini1=Noise_Figure1(i1,i2,i3,m);
                        best_i1=i1;
```

```
                        best_i2=i2;
                        best_i3=i3;
                    end

                end

            else

                INMN=matching_network(i1,i2,1,m);
                Matched_Amp = rfckt.cascade('ckts',{INMN,Unm_Amp});
                analyze(Matched_Amp,freq,ZL,Zs,Z0);
                aux2=Matched_Amp.AnalyzedResult.NF;
                Noise_Figure(i1,i2,m)=max(aux2);
                if (Noise_Figure(i1,i2,m)<mini)
                    mini=Noise_Figure(i1,i2,m);
                    best_i1=i1;
                    best_i2=i2;

                end

            end
        end

    end


    if((m==3) || (m==4) || (m==7) || (m==8))

        Best_INMN=matching_network(best_i1,best_i2,best_i3,m);
        Best_Matched_Amp=rfckt.cascade('ckts',{Best_INMN,Unm_Amp});

        analyze(Best_Matched_Amp,freq,ZL,Zs,Z0);
        Best_NF{m}=Best_Matched_Amp.AnalyzedResult.NF;

        aux1=mean(Best_NF{m});
        if(aux1<mini_aux)
            mini_aux=aux1;
            bnf=Best_INMN;
            bmi=m;
        end
        best_l1(m)=aux(best_i1);
        best_l2(m)=aux(best_i2);
        best_l3(m)=aux(best_i3);



        figure();

        slice(ll1,ll2,ll3,Noise_Figure1(:,:,:,m),aux,aux,aux);
        colormap Jet
        colorbar('SouthOutside')
        shading interp
        caxis([0,2])
        str1=sprintf('Noise Figure depending on the lengths of l1, l2 and l3 for mode %d

        title(str1)
```

```
    figfile = sprintf('NFMN_%d',m);
    saveas(gcf,[pathname,filesep,figfile],'png');
    saveas(gcf,[pathname,filesep,figfile],'fig');



    figure();

    plot(Best_Matched_Amp,'NF')
    hold all
    plot(Unm_Amp,'NF')
    hold off
    legend('NF - Matched','NF - Unmatched','Location','East');
    str2=sprintf('Best Noise Figure obtained with mode %d',m);
    title(str2)

    figfile = sprintf('NF_%d',m);

    saveas(gcf,[pathname,filesep,figfile],'png');
    saveas(gcf,[pathname,filesep,figfile],'fig');


else

    Best_INMN=matching_network(best_i1,best_i2,1,m);
    Best_Matched_Amp=rfckt.cascade('ckts',{Best_INMN,Unm_Amp});
    analyze(Best_Matched_Amp,freq,ZL,Zs,Z0);
    Best_NF{m}=Best_Matched_Amp.AnalyzedResult.NF;
    aux1=mean(Best_NF{m});
    if(aux1<mini_aux)
        mini_aux=aux1;
        bnf=Best_INMN;
        bmi=m;
    end

    best_l1(m)=aux(best_i1);
    best_l2(m)=aux(best_i2);

    figure()

    p1=subplot(211);
    pcolor(l1,l2,Noise_Figure(:,:,m))
    colormap Jet
    colorbar('SouthOutside')
    shading interp
    caxis([0,2])
    str1=sprintf('Noise Figure depending on the lengths of l1 and l2 for mode %d',

    title(str1)

    set(get(p1,'XLabel'),'String','l1 (m)');
    set(get(p1,'YLabel'),'String','l2 (m)');
    subplot(212);
    plot(Best_Matched_Amp,'NF')
```

```
        hold all
        plot(Unm_Amp,'NF')
        hold off
        legend('NF - Matched','NF - Unmatched','Location','East');
        str2=sprintf('Best Noise Figure obtained with mode %d',m);
        title(str2)

        figfile = sprintf('NF_%d',m);

        saveas(gcf,[pathname,filesep,figfile],'png');
        saveas(gcf,[pathname,filesep,figfile],'fig');

    end

end



end
```

MN_output_search.m

```
%MN_output_search.m -> search for the best output matching network
%
%Usage: [bg, bm,best_l1,best_l2] = MN_output_search(MN_num )
%
%       ------------INPUT VARIABLES---------------
%MN_num -> number of matching networks in usage
%
%       ------------OUTPUT VARIABLES--------------
%bg -> matching network with the best gain
%bm -> best matching network number
%best_l1 -> best length for l1
%best_l2 -> best length for l2


function [bg,bm,best_l1,best_l2,best_l3] = MN_output_search1(MN_num)

global aux Zs Z0 ZL Unm_Amp Gain Gain1 freq pathname Best_Gain

%auxiliar variable used on the calculation of the gain



best_l1=zeros(MN_num,1);
best_l2=zeros(MN_num,1);
best_l3=zeros(MN_num,1);                    %only used on MN={3,4,7,8}



%auxiliar variable for the plots
[ll1,ll2,ll3]=meshgrid(aux,aux,aux);        %MN={3,4,7,8}
[l1,l2]=meshgrid(aux,aux);                  %MN={1,2,5,6}
maxi_aux=1;
```

```
for m=1:MN_num

    maxi=1;
    maxi1=1;
    for i1=1:length(aux)

        for i2=1:length(aux)

            if((m==3) || (m==4) || (m==7) || (m==8))

                for i3=1:length(aux)

                    OUTMN=matching_network(i1,i2,i3,m);
                    Matched_Amp = rfckt.cascade('ckts',{Unm_Amp,OUTMN});
                    analyze(Matched_Amp,freq,ZL,Zs,Z0);

                    [data,~,~] = calculate(Matched_Amp,'Gt','dB');


                    Gain1(i1,i2,i3,m)=min((data{1}(:)));

                    if (Gain1(i1,i2,i3,m)>maxi1)
                        maxi1=Gain1(i1,i2,i3,m);
                        best_i1=i1;
                        best_i2=i2;
                        best_i3=i3;
                    end
                end

            else
                OUTMN=matching_network(i1,i2,1,m);
                Matched_Amp = rfckt.cascade('ckts',{Unm_Amp,OUTMN});
                analyze(Matched_Amp,freq,ZL,Zs,Z0);
                %[sp, ~]=extract(Matched_Amp,'S_parameters');

                [data,~,~] = calculate(Matched_Amp,'Gt','dB');
                Gain(i1,i2,m)=min((data{1}(:)));

                if (Gain(i1,i2,m)>maxi)
                    maxi=Gain(i1,i2,m);
                    best_i1=i1;
                    best_i2=i2;

                end
            end

        end

    end

    if((m==3) || (m==4) || (m==7) || (m==8))


        Best_OUTMN=matching_network(best_i1,best_i2,best_i3,m);
        Best_Matched_Amp=rfckt.cascade('ckts',{Unm_Amp,Best_OUTMN});
```

```
    analyze(Best_Matched_Amp,freq,ZL,Zs,Z0);
    [data,~,~] = calculate(Best_Matched_Amp,'Gt','dB');
    Best_Gain{m}=(data{1}(:));

    aux1=mean(Best_Gain{m});

    if(aux1>maxi_aux)
        maxi_aux=aux1;
        bg=Best_OUTMN;
        bm=m;
    end

    best_l1(m)=aux(best_i1);
    best_l2(m)=aux(best_i2);
    best_l3(m)=aux(best_i3);

    figure()

    slice(ll1,ll2,ll3,Gain1(:,:,:,m),aux,aux,aux);
    colormap Jet
    colorbar('SouthOutside')
    caxis([8,15])
    str1=sprintf('Gain depending on the lengths of l1 and l2 for mode %d',m);
    title(str1)


    figfile = sprintf('Gain1_%d',m);

    saveas(gcf,[pathname,filesep,figfile],'png');
    saveas(gcf,[pathname,filesep,figfile],'fig');

    figure()

    plot(Matched_Amp,'Gt')
    hold all
    plot(Unm_Amp,'Gt')
    hold off
    legend('Gt - Matched','Gt - Unmatched','Location','East');
    str2=sprintf('Best Gain obtained with mode %d ',m);
    title(str2)


    figfile = sprintf('Gain2_%d',m);

    saveas(gcf,[pathname,filesep,figfile],'png');
    saveas(gcf,[pathname,filesep,figfile],'fig');

else

    Best_OUTMN=matching_network(best_i1,best_i2,1,m);
    Best_Matched_Amp=rfckt.cascade('ckts',{Unm_Amp,Best_OUTMN});

    analyze(Best_Matched_Amp,freq,ZL,Zs,Z0);
    [data,~,~] = calculate(Best_Matched_Amp,'Gt','dB');
```

```
        Best_Gain{m}=(data{1}(:));
        aux9=mean(Best_Gain{m});

        if(aux9>maxi_aux)
            maxi_aux=aux9;
            bg=Best_OUTMN;
            bm=m;
        end

        best_l1(m)=aux(best_i1);
        best_l2(m)=aux(best_i2);
        figure()



        p1=subplot(211);
        pcolor(l1,l2,Gain(:,:,m))

        colormap Jet
        colorbar('SouthOutside')
        shading interp
        caxis([8,15])

        str1=sprintf('Gain depending on the lengths of l1 and l2 for mode %d',m);
        title(str1)
        set(get(p1,'XLabel'),'String','l1 (m)');
        set(get(p1,'YLabel'),'String','l2 (m)');

        subplot(212);
        plot(Best_Matched_Amp,'Gt')
        hold all

        plot(Unm_Amp,'Gt')

        hold off

        legend('Gain - Matched','Gain - Unmatched','Location','East');
        str2=sprintf('Best Gain obtained with mode %d',m);
        title(str2)


        figfile = sprintf('Gain3_%d',m);

        saveas(gcf,[pathname,filesep,figfile],'png');
        saveas(gcf,[pathname,filesep,figfile],'fig');

    end

end



end
```

This function makes the calculation of the μ stability test.

s_p.m

```
% s_p.m - stability parameter of a two-port
%
% Usage: [mu] = s_p(S)
%
% S = 2x2 scattering matrix of two-port
% necessary and sufficient conditions for stability:
%        mu > 1


function [mu] = s_p(S)

D = det(S);

mu = (1 - abs(S(1,1))^2) / (abs(S(2,2) - D*conj(S(1,1))) + abs(S(1,2)*S(2,1)));

end
```